**Within-host Dynamics of HIV/AIDS**

by

**Xinqi Xie**

B.Sc., University of Victoria, 2018

A Thesis Submitted in Partial Fulfillment of the
Requirements for the Degree of

MASTER OF SCIENCE

in the Department of Mathematics and Statistics

**Within-host Dynamics of HIV/AIDS**

by

**Xinqi Xie**

B.Sc., University of Victoria, 2018

**Supervisory Committee**

---

Dr. Junling Ma, Co-supervisor

(Department of Mathematics and Statistics)

---

Dr. Pauline van den Driessche, Co-supervisor

(Department of Mathematics and Statistics)

## ABSTRACT

This thesis first investigates within-host HIV models for the acute stage. These models incorporate the immune responses and helper T cells produced from the activation of naive CD4 T cells. Because both naive CD4 T cells and helper T cells are susceptible classes, backward bifurcation and bistability may occur. We start with a simple model that ignores the CD8 T cell dynamics, then extend it to include this dynamics. We also extend our model to consider the latent infection of naive CD4 T cells. Backward bifurcation occurs in all these models. We numerically investigate the stability of viral equilibria, and show the bistability caused by backward bifurcation. Increasing the inflow of CTLs prevents the backward bifurcation. With a large homeostatic source of healthy naive CD4 T cells, the disease is easier to establish when the basic reproduction number is less than one. Reducing the reproduction number below one is not sufficient to control the infection of HIV. Secondly, this thesis investigates the development of AIDS caused by viral diversity, as proposed by Wodarz et al. using a model that does not include the details of immune responses. We extend their model to include density dependence, and show that the viral load increases with viral diversity. To study if this result still holds with more realistic HIV dynamics, we incorporate viral diversity into our first model. We conclude theoretically that the total viral load is positively correlated with the number of viral strains, and viral diversity can drive the development of AIDS. We also find that the total CD4 T cell count does not always decrease with viral diversity. Thus further investigation is needed to fully understand the development of AIDS.

# Contents

# List of Tables

# List of Figures

# List of Abbreviations

| | |
|---|---|
| **AIDS** | Acquired Immunodeficiency Syndrome |
| **CTL** | Cytotoxic T Lymphocyte |
| **HIV** | Human Immunodeficiency Viruses |

# ACKNOWLEDGEMENTS

I would like to thank:

**My supervisors, Professors Junling Ma and Pauline van den Driessche,** for their professional assistance on my thesis and always giving necessary support and suggestions.

**Professor Denise Kirschner** for clarification of the data in Hogue et al. [9].

**My thesis external examiner, Professor Libin Rong,** for his constructive comments and recommendations.

**My parents,** for their endless support and unconditional love since childhood.

**Friends,** for all the unforgettable memories we had together.

**All the staff in the department,** for their generosity and the countless help they provided.

# Chapter 1

# Introduction

The human immunodeficiency virus (HIV) destroys human immune systems and eventually causes acquired immunodeficiency syndrome (AIDS). Within-host HIV viral dynamics has three stages [7]. The first is the initial acute stage with a sharp decrease of CD4 T cells and a sharp peak in viral load. The second is a long asymptomatic stage with the viral load fluctuating around the set-point (a stable constant viral load) [7, 13]. In the last stage, patients develop AIDS, their healthy CD4 T cells are depleted and viral load rises quickly.

HIV are RNA virus, which can generate numerous copies by attaching to target cells. Nowak and May, and Rambaut et al. [14, 19] describe the process about how HIV infects a single target cell and produces new virus. After free viral particles encounter the target cells, the viral RNA genome is reverse transcribed to DNA and integrated into the host DNA sequence. Viral particles are then produced in the target cells, and released upon the death of these cells. According to Rambaut et al. [19], viral mutation happens during viral replication. Natural selection allows viral escape from immune responses. Hosts are infected by a single viral strain, thus during the very early stage of infection, viral particles mostly belong to a single viral strain. But during the course of progression, the virus replicates with a high turnover rate and evolves at a fast rate, which greatly diversifies the virus population. The immune response selects for new viral strains with higher virulence. Here, the

virulence is defined as the speed of progression from the chronic phase to AIDS without drug treatment, and is measured by the number of new infections caused by a single infected cell [13]. Thus viral mutations and diversity are crucial points considered in the studies of HIV. In addition to the immune response, drug treatment is a source of natural selection, but this is not studied in this thesis.

The human immune system is another important factor in the studies of HIV. Some published studies describe the role of T cells that are related to the immune responses [14]. There are two types of T cells that are crucial to the HIV immune responses: CD8 T cells and CD4 T cells. Naive (unactivated) CD4 T cells can be activated by antigen presenting cells to become helper T cells [9]. Both naive CD4 T cells and the helper T cells may be infected by the virus. However, Stevenson et al. [23] have argued that T cell activation allows viral genome integration while resting T cells cannot. The helper T cells are crucial to the viral dynamics. The CD8 T cells, as killer cells, are activated by antigen presenting cells then interact with the helper T cells to become the cytotoxic T lymphocytes (CTLs) [9]; this last process is called licensing. When CTLs encounter the infected cells, they produce chemicals to kill infected cells [14].

Simple within-host HIV models include uninfected target cells (a combination of naive, activated CD4 T cells and helper T cells), infected cells, and free virus [17, 25, 27]. The model used by Pankavich et al. [16] to show bistability is a variation of such a model that includes proliferation in uninfected target cells. Pankavich et al. [16] also show that a Hopf bifurcation of the positive equilibrium may occur when the basic reproduction number is greater than unity. A more complex model describing the progression from the chronic phase to AIDS [7] includes uninfected and infected CD4 T cells, uninfected and infected macrophages cells, and virus. This expanded model contains activation and proliferation in healthy CD4 T cells and macrophages. This model shows an exponential increase in the viral load and a decrease in uninfected CD4 T cells when time goes on. However, this model did not contain the CTL immune response explicitly. Some HIV models described in [3, 9, 10, 25, 27, 6, 5] include CTL

responses explicitly. Wodarz and Nowak assume that CTLs proliferate at a constant rate and the development of CTLs depends on the presence of the T helper cells [27]. Some models [10, 9, 11] describe dendritic cells (antigen presenting cells) and discusse how they influence the development of CTLs. After encountering antigen and HIV in periphery, mature dendritic cells migrate to lymph nodes [9, 10]. Authors of some influenza and HIV models including dendritic cells, CD8 T cells and CTLs proposed that virus stimulates immature dendritic cells [9, 11]; they also indicated that mature dendritic cells are used to increase the influx of healthy T cells and cytotoxic T cells in lymph nodes. Mature dendritic cells can activate healthy T cells to become helper T cells, which can help dendritic cell maturation [11] and make mature dendritic cells become licensed dendritic cells [9].

It has been observed that naive CD4 T cells may be infected at a lower rate [2, 23], but the infection is mostly latent, i.e., the infected cells may not produce viral particles [23]. On the other hand, latently infected CD4 cells may still be activated (by antigens including HIV). Several mathematical models [5, 8, 18, 20, 21] consider that latently infected cells cannot release virus before they are activated. However, these models mostly study memory helper T cells, instead of naive CD4 T cells. To study latently infected naive CD4 T cells, we take the idea of the model studied by Doekes et al. [4], which separates infected CD4 T cells into two classes, a latent pool and an actively replicating class.

Wodarz et al. [26] demonstrate a bistability in a model that includes resting, uninfected and infected CD4 T cells. They assume that resting CD4 T cells can be activated but not infected by HIV. Pankavich et al. [16] and Luo et al. [12] generate two similar models including CD4 T cell activation to show the existence of a backward bifurcation. However, these models do not distinguish between the activation of naive CD4 T cells and the proliferation of activated CD4 T cells.

In this thesis, we formulate a within-host HIV model to show that backward bifurcation can be caused by a new susceptible population produced by the activation of naive CD4 T cells. We adapt our model from the Hogue et al. model [9] that

includes interactions among dendritic cells, naive CD4 T cells, helper T cells, naive CD8 T cells and CTLs. This complicated model captures the essential biological processes of HIV dynamics, but also includes the transmission of the virus by dendritic cells, which may not be relevant for the backward bifurcation. Our simplified model incorporates the activation of naive CD4 T cells and proliferation of helper T cells by separating these two classes. The presence of helper T cells has no effect on the basic reproduction number, but it is crucial for the backward bifurcation.

How HIV progress to AIDS is another question we aim to consider. Wodarz and Nowak [27] generate a within-host HIV model that contains viral diversity. Their model shows the existence of a viral threshold when the supply of the viral population is unlimited. When the viral diversity exceeds this threshold, the total viral load is unbounded. We incorporate viral diversity to our model to illustrate that evolution of virus can drive HIV to AIDS, and to investigate if more biologically relevant models may give the same result as Wodarz and Nowak [27].

In Chapter 2, we develop a simple within-host HIV model to capture the interaction between activation of naive CD4 cells and viral dynamics, while ignoring the biological complexity such as the dynamics of antigen presenting cells and CD8 T cells. We show that the existence of helper T cells can cause a backward bifurcation in our model. However, this model has less biological meanings when we ignore the latent infection in the acute stage. In Chapter 3, an extended model with the activation of the latently infected CD4 T cells by foreign pathogens is developed. We demonstrate that backward bifurcation may also occur in this model. The results in Chapters 2 and 3 are published in [28].

In Chapter 4, we revise the Wodarz and Nowak model [27] to show that the strain-specific immunity is crucial for the progression to AIDS, but the group-specific immunity is not. In addition, we show that, with a viral carrying capacity, the viral load still increases with viral diversity, but there is no threshold diversity that leads to AIDS. In Chapter 5, we add viral diversity to our 4-dimensional model in Chapter 2. We illustrate that the viral population is still bounded because of a constant supply

of CD4 T cells, and the viral population at endemic equilibrium is a positive function of viral diversity. A summary of our conclusions is given in Chapter 6.

# Chapter 2

# Within-host Model for the Acute Stage of HIV

A simple within-host HIV model that includes uninfected target cells $T$, infected cells $I$, and free virus $V$ are derived to illustrate the dynamics of virus at the acute stage [17, 27]. The model shows below,

$$\frac{dT}{dt} = \lambda - \beta VT - d_T T, \tag{2.1a}$$

$$\frac{dI}{dt} = \beta VT - d_I I, \tag{2.1b}$$

$$\frac{dV}{dt} = pI - d_V V. \tag{2.1c}$$

where $\lambda$ denotes the source of T cells. Target cells are infected by free virus at a rate $\beta$, and free viral particles are released from infected cells immediately at a rate $p$ after uninfected cells are infected by a free virus and die. $d_T$, $d_I$ and $d_V$ are death rate of target cells, infected cells and virus respectively. When $\mathcal{R}_0 = \frac{p\lambda\beta}{d_T d_I d_V} < 1$, virus will not spread out and are controlled by the immune response system [17, 27]. However when $\mathcal{R}_0 > 1$, the total viral load increases dramatically to a peak, then decreases to an equilibrium within few weeks because of the limit of supply of target cells [17, 27]. This model only describes the kinetics of virus at the acute stage. Because of the complicated mechanism of HIV infection, this model is too simple to

analyze the dynamics of virus. Thus we consider the effects of immune responses and T helper cells which are infected and activated by virus. Both healthy naive CD4 T cells and T helper cells are susceptible to HIV, while the simple model (2.1) only has one susceptible class.

## 2.1 Within-host HIV Model with Naive CD4 T Cells and Helper T Cells

Because activated CD4 T cells are more commonly infected by virus, in this chapter, we build a simple within-host HIV model (a simplification of Hogue et al. [9]) that includes the key features of CD4 T cell activation and viral dynamics. Our model includes healthy naive CD4 T cells ($\tilde{T}_4$), helper T cells ($\tilde{T}_H$), infected CD4 T cells ($\tilde{I}$) and virus ($\tilde{V}$). The model flowchart is shown in Figure 2.1.

In this model naive CD4 T cells $\tilde{T}_4$ are produced at a constant rate $S_4$ and die at a constant rate $\tilde{\mu}_4$, assumptions that guarantee a bounded $\tilde{T}_4$ population. For simplification, our model does not include antigen presenting cells. We assume that $\tilde{T}_4$ cells are activated at a rate $\tilde{r}_4\tilde{T}_4\tilde{V}$. The infection rates of $\tilde{T}_4$ and $\tilde{T}_H$ cells are $\tilde{\beta}_4$ and $\tilde{\beta}_H$, respectively. The homeostatic proliferation rate of $\tilde{T}_H$ is $\tilde{p}_H$, which is assumed to be less than the death rate of $\tilde{T}_H$ cells, $\tilde{\mu}_H$, to guarantee a bounded $\tilde{T}_H$ population. Infected cells die at a constant rate $\tilde{\mu}_I$, and each dead cell releases $N$ free viral particles. In addition, infected cells are killed by CTLs at a constant rate $\tilde{\kappa}_I$. The CTL population is positively related to the licensed dendritic cells and T helper cells, which are both positively related to viral load [9, 6, 5]. Thus, we simply assume that the CTL population $\tilde{T}_C$ is proportional to the T helper cells, i.e., $\tilde{T}_C = \rho\tilde{T}_H$, and our model ignores the dynamics of CTLs. Free virus die at a constant rate $\tilde{\mu}_V$. Our

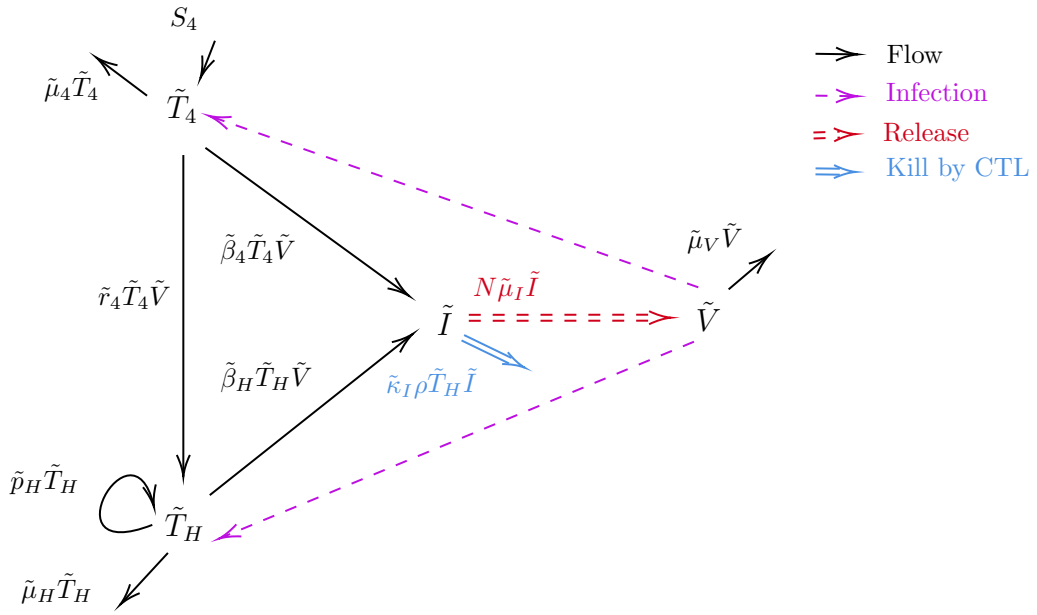


Figure 2.1: Progression diagram for the within-host HIV model (1).

model is given by the following four-dimensional system.

$$\frac{d\tilde{T}_4}{d\tau} = S_4 - \tilde{r}_4\tilde{T}_4\tilde{V} - \tilde{\beta}_4\tilde{T}_4\tilde{V} - \tilde{\mu}_4\tilde{T}_4, \tag{2.2a}$$

$$\frac{d\tilde{T}_H}{d\tau} = \tilde{r}_4\tilde{T}_4\tilde{V} - \tilde{\beta}_H\tilde{T}_H\tilde{V} - \tilde{\mu}_H\tilde{T}_H + \tilde{p}_H\tilde{T}_H, \tag{2.2b}$$

$$\frac{d\tilde{I}}{d\tau} = \tilde{\beta}_H\tilde{T}_H\tilde{V} + \tilde{\beta}_4\tilde{T}_4\tilde{V} - \tilde{\mu}_I\tilde{I} - \tilde{\kappa}_I\rho\tilde{T}_H\tilde{I}, \tag{2.2c}$$

$$\frac{d\tilde{V}}{d\tau} = N\tilde{\mu}_I\tilde{I} - \tilde{\mu}_V\tilde{V}. \tag{2.2d}$$

The parameters of model (2.2) are listed in Table 2.1. The initial conditions satisfy $\tilde{T}_4(0) > 0$, $\tilde{T}_H(0) \geq 0$, $\tilde{I}(0) \geq 0$ and $\tilde{V}(0) > 0$. We assume that all parameters are positive with $\tilde{\mu}_H > \tilde{p}_H$.

To reduce the number of parameters, we derive the non-dimensional form of our model by setting $\tilde{T}_4 = S_4T_4/\tilde{\mu}_4$, $\tilde{T}_H = S_4T_H/\tilde{\mu}_4$, $\tilde{I} = S_4I/\tilde{\mu}_4$, $\tilde{V} = NS_4V/\tilde{\mu}_4$, $\tau = t/\tilde{\mu}_V$, $\tilde{\kappa}_I = \kappa_I\tilde{\mu}_4\tilde{\mu}_V/S_4$, $\tilde{r}_4 = r_4\tilde{\mu}_4\tilde{\mu}_V/(NS_4)$, $\tilde{\beta}_H = \beta_H\tilde{\mu}_4\tilde{\mu}_V/(NS_4)$, $\tilde{\beta}_4 = \beta_4\tilde{\mu}_4\tilde{\mu}_V/(NS_4)$, $\tilde{\mu}_I = \mu_I\tilde{\mu}_V$, $\tilde{\mu}_4 = \mu_4\tilde{\mu}_V$, $\tilde{\mu}_H = \mu_H\tilde{\mu}_V$ and $\tilde{p}_H = p_H\tilde{\mu}_V$. Thus, our non-dimensional model with the non-dimensional variables for within-host HIV model is

| **Parameter** | **Meaning** |
|---|---|
| $\tilde{\mu}_4$ | Rate of removal of naive CD4 T cells |
| $\tilde{r}_4$ | Activation rate of naive CD4 T cells by the presence of virus |
| $\tilde{\beta}_4$, $\tilde{\beta}_H$ | Infection rate of naive CD4 T cells and helper T cells by virus respectively |
| $\tilde{\kappa}_I$ | Killing rate of infected cells by CTL |
| $\tilde{\mu}_I$ | Rate of releasing viral particles from infected cells |
| $\tilde{\mu}_H$, $\tilde{\mu}_V$ | Natural death rate of helper T cells and virus respectively |
| $\tilde{p}_H$ | Proliferation rate of helper T cells |
| $\rho$ | $\rho\tilde{T}_H$ is the CTL count |
| $N$ | Average virus produced by an infected cell |
| $S_4$ | Homeostatic source of healthy naive CD4 T cells |

Table 2.1: Summary of parameters of model (2.2).

given by the following system.

$$\begin{aligned}
\frac{dT_4}{dt} &= \mu_4 - r_4 T_4 V - \beta_4 T_4 V - \mu_4 T_4, && \text{(2.3a)}\\
\frac{dT_H}{dt} &= r_4 T_4 V - \beta_H T_H V - \mu_H T_H + p_H T_H, && \text{(2.3b)}\\
\frac{dI}{dt} &= \beta_H T_H V + \beta_4 T_4 V - \mu_I I - \kappa_I \rho T_H I, && \text{(2.3c)}\\
\frac{dV}{dt} &= \mu_I I - V. && \text{(2.3d)}
\end{aligned}$$

In the limiting case where $\beta_4 = 0$, $\kappa_I = 0$, and $V \propto I$, this model reduces to the Wodarz et al. [26, Section 3].

## 2.2 Disease-free Equilibrium

In this section, we consider the existence of equilibria for model (2.3) and compute the viral basic reproduction number $\mathcal{R}_0$ of this model. Biologically, the viral basic reproduction number is the number of susceptible cells that are infected by a single infected cell. The nondimensional model (2.3) has a virus-free equilibrium: $E^0 = (T_4^0, T_H^0, I^0, V^0) = (1, 0, 0, 0)$. The Jacobian matrix obtained by linearization at the virus-free equilibrium is

$$J_0 = \begin{pmatrix} -\mu_4 & 0 & 0 & -(r_4 + \beta_4) \\ 0 & -d_H & 0 & r_4 \\ 0 & 0 & -\mu_I & \beta_4 \\ 0 & 0 & \mu_I & -1 \end{pmatrix}, \qquad (2.4)$$

where $d_H = \mu_H - p_H > 0$.

The eigenvalues of $J_0$ are $-\mu_4 < 0$, $-\mu_H + p_H < 0$ and solutions of the quadratic equation

$$\lambda^2 + (\mu_I + 1)\lambda + \mu_I(1 - \beta_4) = 0, \qquad (2.5)$$

Solutions of (2.5) are negative if and only if $1 - \beta_4 > 0$. Thus

$$\mathcal{R}_0 = \beta_4 = \frac{\tilde{\beta}_4 N S_4}{\tilde{\mu}_V \tilde{\mu}_4},$$

which means a single infected cell is expected to infect on average $\mathcal{R}_0 = \beta_4$ naive CD4 T cells. The fraction $\tilde{\beta}_4 S_4/\tilde{\mu}_4$ is the infection rate of naive CD4 T cells when the disease-free population size of CD4 T cells is $S_4/\tilde{\mu}_4$. An infected cell can produce $N/\tilde{\mu}_V$ virus on average during the viral lifespan $1/\tilde{\mu}_V$. If $\mathcal{R}_0 < 1$, then the virus-free equilibrium is locally asymptotically stable. If $\mathcal{R}_0 > 1$, then the virus-free equilibrium is unstable, and initially the virus grows exponentially. Furthermore, helper T cells, as an alternate viral target along with CD4 T cells, cannot affect the value of $\mathcal{R}_0$. Thus, preventing activation of naive CD4 T cells and reducing the infection rate of helper T cells cannot eliminate the within-host HIV.

## 2.3 Endemic Equilibria

Endemic equilibria satisfy the system (2) with derivatives set to zero. Then the endemic equilibrium values for $T_4$, $T_H$ and $I$ in terms of $V$ are

$$\begin{aligned} T_4^* &= \frac{\mu_4}{\mu_4 + r_4 V^* + \beta_4 V^*}, \\ T_H^* &= \frac{r_4 T_4^* V^*}{\beta_H V^* + \mu_H - p_H}, \\ I^* &= \frac{V^*}{\mu_I}. \end{aligned}$$

The endemic equilibria for $V$ satisfies

$$AV^{*2} + BV^* + C = 0, \tag{2.6}$$

where

$$A = \mu_I \beta_H (r_4 + \beta_4), \tag{2.7a}$$

$$B = \mu_I \mu_4 \beta_H (1 - r_4 - \beta_4) + \mu_I (r_4 + \beta_4) d_H + \kappa_I \rho \mu_4 r_4, \tag{2.7b}$$

$$C = \mu_I \mu_4 d_H (1 - \beta_4). \tag{2.7c}$$

It is clear that all coefficients $A$, $B$ and $C$ depend on $\mathcal{R}_0 = \beta_4$, thus, the signs of the roots of the quadratic equation (2.6) depend on the value of $\mathcal{R}_0$ as well as other parameter values.

In the limiting case that results in the Wodarz et al. [26, Section 3] model, $\mathcal{R}_0 = 0$ and there may exist two positive equilibria if $r_4 > 1$ (giving $B < 0$ and $C > 0$). This may result in the bistability shown in Wodarz et al. [26, Section 3].

## 2.4 Backward Bifurcation

We can verify that if $\mathcal{R}_0 = 1$ and there are no helper cells present, meaning that $r_4 = 0$, then $A$, $B$ and $C$ of equation (2.6) are all positive, so there is no positive root $V^*$ satisfying equation (2.6). We obtain the same result when $\mathcal{R}_0 = 1$ and $T_H$ are not infected by virus, i.e, $\beta_H = 0$.

When $\mathcal{R}_0$ is the bifurcation parameter in this model, let $\mathbf{v}^\top$ and $\mathbf{w}$ be the left and right eigenvectors at eigenvalue zero of (2.4) respectively at $\mathcal{R}_0 = 1$ with $\mathbf{v}^\top \mathbf{w} = 1$, and $E^0$ be the disease-free equilibrium. As in [1, 24], let

$$
\begin{aligned}
a &= \frac{1}{2} \sum_{i,j,k=1}^{4} v_i w_j w_k \frac{\partial^2 f_i}{\partial x_j \partial x_k}(E^0, 1) \\
&= \frac{\mu_I}{2(\mu_I + 1)} \left[ \frac{r_4 \beta_H}{\mu_H - p_H} - \frac{r_4 + 1}{\mu_4} - \frac{r_4 \kappa_I \rho}{\mu_I d_H} \right], \qquad (2.8a) \\
b &= \sum_{i,j=1}^{4} v_i w_j \frac{\partial^2 f_i}{\partial x_j \partial \mathcal{R}_0}(E^0, 1) = \frac{\mu_I}{\mu_I + 1}, \qquad (2.8b)
\end{aligned}
$$

where $x = (x_1, x_2, x_3, x_4)^\top = (T_4, T_H, I, V)^\top$ and $f_i = dx_i/dt$ from model (2.3). Note that signs of $a$ and $b$ determine the type and direction of bifurcation. From the proof of the Theorem 1, $b$ is always positive, and the expression for $a$ is proved.

**Theorem 1.** *Consider the within-host HIV model defined by (2) with $a$ and $b$ defined in (2.8). Then*

- *if $a > 0$, there exists a backward bifurcation at $\mathcal{R}_0 = 1$;*
- *if $a < 0$, there exists a forward bifurcation at $\mathcal{R}_0 = 1$.*

*Proof.* In our model, there are four compartments. As we defined previously, $x = (x_1, x_2, x_3, x_4)^\top = (T_4, T_H, I, V)^\top$ and $f_i = dx_i/dt$. Our model satisfies the conditions

A1- A5 defined in [1, 24]. Note that $E^0 = (T_4^0, T_H^0, I^0, V^0) = (1, 0, 0, 0)$ is always an equilibrium. Linearization of system (2.3) at the bifurcation point $\mathcal{R}_0 = 1$ gives

$$J = \begin{pmatrix} -\mu_4 & 0 & 0 & -(r_4+1) \\ 0 & -(\mu_H - p_H) & 0 & r_4 \\ 0 & 0 & -\mu_I & 1 \\ 0 & 0 & \mu_I & -1 \end{pmatrix}.$$

This matrix has eigenvalues $-\mu_4$, $-(\mu_H - p_H)$, $-(\mu_I + \beta_4)$ and 0. The left eigenvector $\mathbf{v}^\top$ and right eigenvector $\mathbf{w}$ at eigenvalue zero are

$$\mathbf{v} = \begin{pmatrix} 0 \\ 0 \\ \frac{\mu_I}{\mu_I+1} \\ \frac{\mu_I}{\mu_I+1} \end{pmatrix}, \quad \mathbf{w} = \begin{pmatrix} -\frac{(r_4+1)}{\mu_4} \\ \frac{r_4}{\mu_H - p_H} \\ \frac{1}{\mu_I} \\ 1 \end{pmatrix}.$$

The backward bifurcation theorems in [1, 24] guarantee that, if

$$b = \sum_{i,j=1}^{4} v_i w_j \frac{\partial^2 f_i}{\partial x_j \partial \mathcal{R}_0}(E^0, 1) > 0,$$

and

$$a = \frac{1}{2} \sum_{i,j,k=1}^{4} v_i w_j w_k \frac{\partial^2 f_i}{\partial x_j \partial x_k}(E^0, 1) > 0,$$

then a backward bifurcation occurs at $\mathcal{R}_0 = 1$. Otherwise, if $b > 0$ and $a < 0$, then there is no backward bifurcation.

The nonzero second derivatives used to compute $b$ are

$$\begin{aligned} \frac{\partial^2 f_1}{\partial x_4 \partial \mathcal{R}_0}(E^0, 1) &= -1, \\ \frac{\partial^2 f_3}{\partial x_4 \partial \mathcal{R}_0}(E^0, 1) &= 1. \end{aligned}$$

Thus,

$$b = v_1 w_4 \frac{\partial^2 f_1}{\partial x_4 \partial \mathcal{R}_0}(E^0, 1) + v_3 w_4 \frac{\partial^2 f_3}{\partial x_4 \partial \mathcal{R}_0}(E^0, 1) = \frac{\mu_I}{\mu_I + 1} > 0.$$

The nonzero second derivatives used to compute $a$ are

$$\begin{aligned}
\frac{\partial^2 f_1}{\partial x_1 \partial x_4}(E^0,1) &= -(r_4+1),\\
\frac{\partial^2 f_2}{\partial x_1 \partial x_4}(E^0,1) &= r_4,\\
\frac{\partial^2 f_2}{\partial x_2 \partial x_4}(E^0,1) &= -\beta_H,\\
\frac{\partial^2 f_3}{\partial x_2 \partial x_4}(E^0,1) &= \beta_H,\\
\frac{\partial^2 f_3}{\partial x_1 \partial x_4}(E^0,1) &= 1,\\
\frac{\partial^2 f_3}{\partial x_2 \partial x_3}(E^0,1) &= -\rho\kappa_I.
\end{aligned}$$

Thus,

$$\begin{aligned}
a &= \frac{1}{2}\left[v_1 w_1 w_4 \frac{\partial^2 f_1}{\partial x_1 \partial x_4}(E^0,1) + v_2 w_1 w_4 \frac{\partial^2 f_2}{\partial x_1 \partial x_4}(E^0,1) + v_2 w_2 w_4 \frac{\partial^2 f_2}{\partial x_2 \partial x_4}(E^0,1)\right.\\
&\quad \left. + v_3 w_2 w_4 \frac{\partial^2 f_3}{\partial x_2 \partial x_4}(E^0,1) + v_3 w_1 w_4 \frac{\partial^2 f_3}{\partial x_1 \partial x_4}(E^0,1) + v_3 w_2 w_3 \frac{\partial^2 f_3}{\partial x_2 \partial x_3}(E^0,1)\right]\\
&= \frac{\mu_I}{2(\mu_I+1)}\left[\frac{r_4\beta_H}{\mu_H - p_H} - \frac{r_4+1}{\mu_4} - \frac{r_4\rho\kappa_I}{\mu_I d_H}\right].
\end{aligned}$$

□

**Remark 1.** *From (2.7) and (2.8), the backward bifurcation condition $a > 0$ is equivalent to $B < 0$ with $\mathcal{R}_0 = \beta_4 = 1$.*

If either $r_4 = 0$ or $\beta_H = 0$, then the backward bifurcation condition is not satisfied. We can conclude that the backward bifurcation can exist only when helper cells are present, that is helper cells are a second susceptible class to HIV.

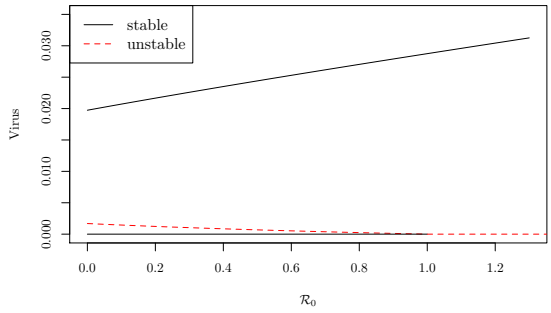


(a) Bistability when $\rho = 1.1525$

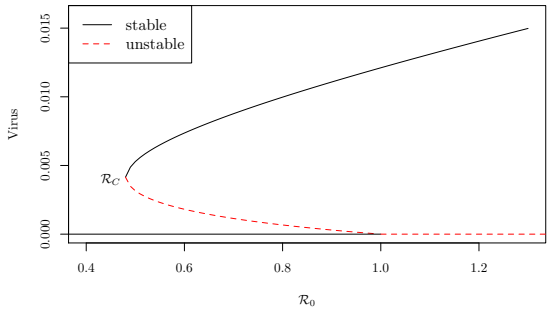


(b) Backward bifurcation when $\rho = 1.1575$

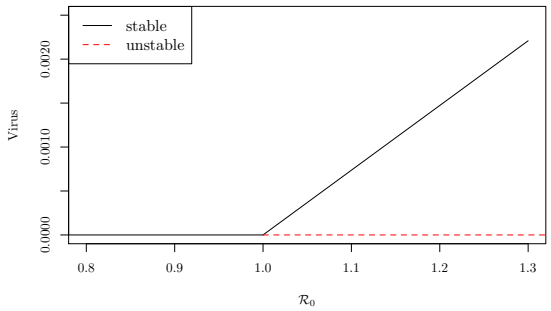


(c) Forward bifurcation when $\rho = 1.1625$

Figure 2.2: Bifurcation diagrams of the disease free equilibrium of equation (2.3), and the stability illustrated numerically, where $\mu_4 = 3.875$, $\beta_H = 525$, $r_4 = 525$, $\kappa_I = 1750$, $\mu_I = 3.875$, $\mu_H = 3.875$, $p_H = 1.5$. All parameter values come from Hogue et al. model [9] except $\beta_H$ and $\rho$.

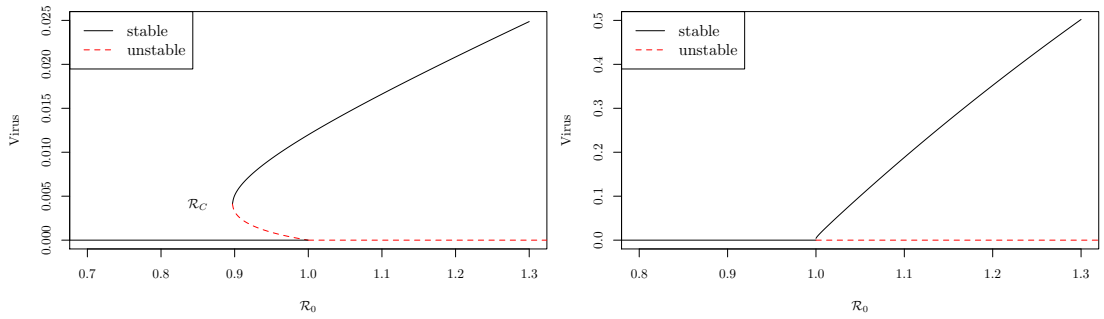


(a) Backward bifurcation when $\tilde{r}_4 = 4 \times 10^{-10}$, $S_4 = 5425 \times 10^5$ giving $r_4 = 105$

(b) Forward bifurcation when $\tilde{r}_4 = 4 \times 10^{-12}$, $S_4 = 5425 \times 10^5$ giving $r_4 = 1.05$

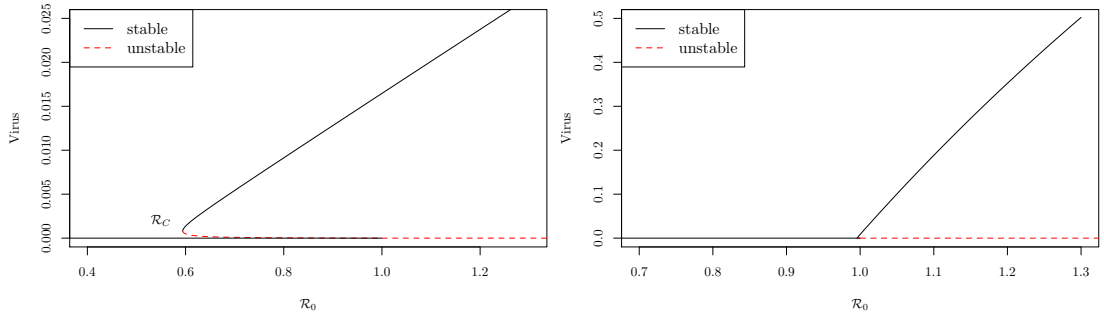


(c) Backward bifurcation when $\tilde{r}_4 = 4 \times 10^{-12}$, $S_4 = 5425 \times 10^7$ giving $r_4 = 105$

(d) Forward bifurcation when $\tilde{r}_4 = 4 \times 10^{-14}$, $S_4 = 5425 \times 10^7$ giving $r_4 = 1.05$

Figure 2.3: Bifurcation diagrams of the equilibria of (2.3) with $\mathcal{R}_0$ as the bifurcation parameter. A large $r_4$ value causes backward bifurcation, while a large $S_4$ value reduces the attractive basin of the disease free equilibrium. In the Hogue et al. model $S_4 = 5425 \times 10^5$. We pick $\rho = 1.1575$. The other parameter values are the same as in Figure 2.2 except $r_4$ and $\tilde{r}_4$.

Figure 2.2 illustrates the dynamics of virus with change of $\mathcal{R}_0$ of the nondimensional model (2.3). We pick dimensional parameters $\tilde{\mu}_4$, $\tilde{\mu}_I$, $\tilde{\mu}_H$, $\tilde{r}_4$, $\tilde{\kappa}_I$ and $\tilde{p}_H$ from Hogue et al. model [9] to generate nondimensional parameters. We solve the equilibrium viral load $V^*$ from (2.6), and determine the stability numerically using the eigenvalues of the Jacobian. We vary $\rho$ to study the change in the bifurcation diagram.

In Figure 2.2a, when $\rho = 1.1525$, the population of virus is bistable when $\mathcal{R}_0 < 1$, which means a locally asymptotically stable endemic equilibrium and disease equilibrium coexist. After increasing $\rho$ slightly to 1.1575, there exists a backward bifurcation. Two endemic equilibria exist together with the locally asymptotically stable disease-free equilibrium when $\mathcal{R}_0$ is in the range $\mathcal{R}_C < \mathcal{R}_0 < 1$. When $\mathcal{R}_0 < \mathcal{R}_C$, there only exists a disease-free equilibrium. When $\mathcal{R}_0 > 1$, the disease persists. Figure 2.2c shows that when $\rho = 1.1625$, the dynamics of the virus is a forward bifurcation instead of a backward bifurcation. For this larger $\rho$ value, the disease dies out when $\mathcal{R}_0 < 1$, but the virus is out of control when $\mathcal{R}_0 > 1$. Figure 2.2 shows that backward bifurcation does not happen with a larger value of $\rho$, which indicates that a stronger immune responses of CTL cells can prevent backward bifurcation. Increasing $\kappa_I$ has the same effect as increasing $\rho$.

Figure 2.3 shows the bifurcation diagram of Model (2.3) by numerically solving the equilibrium viral load from (2.6). We mainly use the parameter values of Hogue et al. [9] for our model, we pick $\rho = 1.1575$, and vary $S_4$ and $r_4$. When $S_4$ is the homeostatic source of healthy CD4 T cells and $r_4 = \tilde{r}_4 N S_4/(\tilde{\mu}_V \tilde{\mu}_4)$, increasing $S_4$ results in easier activation from CD4 T cells by virus, which enhances the inflow of helper T cells. Figure 2.3 shows that, with a large $r_4$, backward bifurcation occurs for $\mathcal{R}_C < \mathcal{R}_0 < 1$, where $\mathcal{R}_C$ is the critical value of $\mathcal{R}_0$ for some parameter values. Depending on the initial conditions, the virus may persist or die out. For small $r_4$, there is no backward bifurcation. Numerical simulations also show that, if backward bifurcation occurs, the larger endemic equilibrium is locally asymptotically stable while the smaller one is unstable. If $\mathcal{R}_0 < \mathcal{R}_C$, there only exists the linearly stable disease-free equilibrium. If $\mathcal{R}_0 > 1$, the system has only one locally asymptotically stable endemic equilibrium and an unstable disease-free equilibrium.

Numerically, larger values of $S_4$ cause backward bifurcation for a larger range of $\mathcal{R}_0$. Increasing the value of $S_4$ from $5425 \times 10^5$ to $5425 \times 10^7$, the vertex of the parabola like curve is closer to the origin and the unstable endemic equilibrium curve is flatter when $\mathcal{R}_0 < 1$. Due to the large count of naive CD4 T cells in the body

[9], i.e., large $S_4$, the branch of the unstable equilibrium will be very close to the disease free equilibrium. In this case, $\mathcal{R}_C$ is approximately the threshold for disease persistence, independent of the initial conditions.

## 2.5 An Extended Model with CTL Dynamics

We have shown in Section 4 that the existence of helper T cells may cause backward bifurcation. In this Section, we extended our four-dimensional model to a six-dimensional model that includes the dynamics of CTLs, rather than simply setting CTLs proportional to virus. Our six-dimensional model contains two more classes: healthy CD8 T cells ($\tilde{T}_8$) and CTLs ($\tilde{T}_C$). Because CD8 T cells are primed to become CTLs by antigen-presenting licensed dendritic cells that are defined as mature dendritic cells encountered with helper T cells [9], we can ignore the class of dendritic cells and simply assume that CD8 T cells are activated by helper T cells at a constant rate $\tilde{r}_8$. There exists a constant homeostatic proliferation rate $S_8$ of naive CD8 T cells. Naive CD8 T cells die at a rate $\tilde{\mu}_8$, and CTLs proliferate at a constant rate $\tilde{p}_C$, and die at a rate $\tilde{\mu}_C > \tilde{p}_C$. The meaning of the parameters is shown in Table 2.2. The extended is given by the following system, with nonnegative initial conditions.

$$\frac{d\tilde{T}_4}{dt} = S_4 - \tilde{r}_4\tilde{T}_4\tilde{V} - \tilde{\beta}_4\tilde{T}_4\tilde{V} - \tilde{\mu}_4\tilde{T}_4, \tag{2.9a}$$

$$\frac{d\tilde{T}_H}{dt} = \tilde{r}_4\tilde{T}_4\tilde{V} - \tilde{\beta}_H\tilde{T}_H\tilde{V} - \tilde{\mu}_H\tilde{T}_H + \tilde{p}_H\tilde{T}_H, \tag{2.9b}$$

$$\frac{d\tilde{I}}{dt} = \tilde{\beta}_H\tilde{T}_H\tilde{V} + \tilde{\beta}_4\tilde{T}_4\tilde{V} - \tilde{\mu}_I\tilde{I} - \tilde{\kappa}_I\tilde{T}_C\tilde{I}, \tag{2.9c}$$

$$\frac{d\tilde{V}}{dt} = N\tilde{\mu}_I\tilde{I} - \tilde{\mu}_V\tilde{V}, \tag{2.9d}$$

$$\frac{d\tilde{T}_8}{dt} = S_8 - \tilde{r}_8\tilde{T}_8\tilde{T}_H - \tilde{\mu}_8\tilde{T}_8, \tag{2.9e}$$

$$\frac{d\tilde{T}_C}{dt} = \tilde{r}_8\tilde{T}_8\tilde{T}_H + \tilde{p}_C\tilde{T}_C - \tilde{\mu}_C\tilde{T}_C. \tag{2.9f}$$

Note that this model has the same viral basic reproduction number $\mathcal{R}_0 = \frac{\tilde{\beta}_4 N S_4}{\tilde{\mu}_V\tilde{\mu}_4}$ as the four-dimensional model (2.2).

| Parameter | Meaning |
|---|---|
| $\tilde{\mu}_4$ | Rate of removal of naive CD4 T cells |
| $\tilde{r}_4$ | Activation rate of naive CD4 T cells by the presence of virus |
| $\tilde{r}_8$ | Activation rate of CD8 T cells by helper T cells |
| $\tilde{\beta}_4$, $\tilde{\beta}_H$ | Infection rate of naive CD4 T cells and helper T cells by virus respectively |
| $\tilde{\kappa}_I$ | Killing rate of infected cells by CTL |
| $\tilde{\mu}_I$ | Rate of releasing viral particles from infected cells |
| $\tilde{\mu}_H$, $\tilde{\mu}_V$, $\tilde{\mu}_8$, $\tilde{\mu}_C$ | Natural death rate of helper T cells, virus, CD8 T cells and CTLs respectively |
| $\tilde{p}_H$, $\tilde{p}_C$ | Proliferation rate of helper T cells and CTLs respectively |
| $N$ | Average virus produced by an infected cell |
| $S_4$ | Homeostatic source of healthy CD4 T cells |
| $S_8$ | Homeostatic source of healthy CD8 T cells |

Table 2.2: Summary of parameters of model (2.9).

We numerically evaluate the nonnegative equilibria, and determine their stability for model (2.9). Figure 2.4 shows the bifurcation diagrams of the disease free equilibrium. All parameters used in Figure 2.4b come from Hogue et al. [9] except $\tilde{r}_4$ and $\tilde{r}_8$. In addition, we set $\tilde{\beta}_4 = \tilde{\beta}_H$. For Figure 2.4a, the same parameters are used except that $S_8$ is decreased. Backward bifurcation may occur. However, increasing $S_8$, i.e., increasing the inflow of $\tilde{T}_C$ prevents the backward bifurcation from occurring. Intuitively this is because increasing equilibrium $\tilde{T}_C$ in this model is equivalent to increasing $\tilde{\kappa}_I$ in model (2.2).

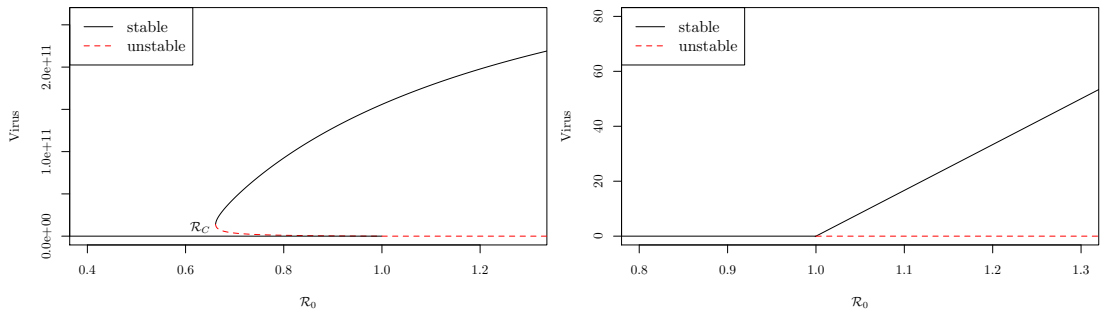


(a) Backward bifurcation $S_8 = 186$ (b) Forward bifurcation $S_8 = 186 \times 10^6$

Figure 2.4: Bifurcation diagrams of the equilibria of (2.9) with $\mathcal{R}_0$ as the bifurcation parameter, where $\tilde{\beta}_4 = \tilde{\beta}_H$, $S_4 = 3.5 \times 10^8 \times 1.55$, $\tilde{\mu}_4 = 1.55$, $\tilde{\mu}_H = 1.55$, $\tilde{\mu}_I = 1.55$, $\tilde{\mu}_8 = 1.55$, $\tilde{\mu}_C = 1.55$, $\tilde{\mu}_V = 0.4$, $\tilde{p}_H = \tilde{p}_C = 0.6$, $N = 300$, $\tilde{\kappa}_I = 2 \times 10^{-6}$, $\tilde{r}_4 = 10^{-9}$, $\tilde{r}_8 = 10^{-4}$.

## 2.6 Concluding Remarks

The main purpose of this chapter is verifying theoretically the possible existence of backward bifurcation. The backward bifurcation may be caused by the activation and proliferation of naive CD4 T cells to become helper T cells, because this process creates a new susceptible population only in the presence of the virus. We create a simple model that considers the activation and proliferation process, keeping track of the naive CD4 T cells, the helper T cells, infected cells and the viral load. We use viral load as an proxy for antigen presenting cells and CTLs. Bifurcation analysis shows that backward bifurcation may indeed occur in our simple model. We then extend our model to keep track of the CTL dynamics, and the extended model also shows backward bifurcation. The bifurcation condition that we derived shows that, if the helper T cells are not produced ($r_4 = 0$) or if they are not susceptible ($\beta_H = 0$), then backward bifurcation cannot occur. This confirms that the susceptible helper T cell population indeed enables the backward bifurcation.

The backward bifurcation condition suggests that a small difference between death

rate and proliferation rate of helper T cells ($\mu_H - p_H$) can promote backward bifurcation, because it gives a large equilibrium of the helper T cell population, i.e., it gives a large susceptible population size with the presence of the virus. On the other hand, a large value of the killing rate of infected cells by CTLs ($\kappa_I$) makes the backward bifurcation less likely to occur. When $\mathcal{R}_0$ is between $\mathcal{R}_C$ and 1, the model dynamics depend on the initial values.

# Chapter 3

# A Model for Within-host HIV with Latent Infection

In the last chapter, we demonstrated the viral dynamics without drug therapy in the acute phase when the helper T cells act as the second susceptible class, and showed the presence of the backward bifurcation. In this chapter, based on the model (2.2), we construct a 5-dimensional model with latent infection in the acute phase to describe the dynamics of virus. We include naive CD4 T cells that are latently infected, and only release virus after being activated. It is possible that the backward bifurcation still exists and the existence of backward bifurcation depends on the parameter values.

## 3.1 Model Formulation

It has been observed [23] that naive CD4 T cells may be infected by HIV at a much lower rate than helper T cells. However, the infected naive CD4 T cells are latent, i.e., they do not produce viral particles, but they may be activated and then produce viral particles.

To make our simple within-host HIV model (2.3) more biological meaningful, we extend it to include latently infected CD4 T cells, and introduce a new variable $\tilde{I}_4$ for these cells. Here $\tilde{I}_H$ represents both the infected helper T cells and the activated

latently infected CD4 T cells. The $\tilde{I}_4$ cells may be activated by HIV antigens at a rate $\tilde{r}_4$, and other antigens at a rate $\sigma$. Viral particles are only produced by $\tilde{T}_H$ cells. This latent infection model is given below with nonnegative initial conditions.

$$\frac{d\tilde{T}_4}{d\tau} = S_4 - \tilde{r}_4\tilde{T}_4\tilde{V} - \tilde{\beta}_4\tilde{T}_4\tilde{V} - \tilde{\mu}_4\tilde{T}_4, \tag{3.1a}$$

$$\frac{d\tilde{T}_H}{d\tau} = \tilde{r}_4\tilde{T}_4\tilde{V} - \tilde{\beta}_H\tilde{T}_H\tilde{V} - \tilde{\mu}_H\tilde{T}_H + \tilde{p}_H\tilde{T}_H, \tag{3.1b}$$

$$\frac{d\tilde{I}_4}{d\tau} = \tilde{\beta}_4\tilde{T}_4\tilde{V} - \tilde{r}_4\tilde{I}_4\tilde{V} - \tilde{\kappa}_I\rho\tilde{T}_H\tilde{I}_4 - \tilde{\sigma}\tilde{I}_4 - \tilde{\mu}_I\tilde{I}_4, \tag{3.1c}$$

$$\frac{d\tilde{I}_H}{d\tau} = \tilde{r}_4\tilde{I}_4\tilde{V} + \tilde{\beta}_H\tilde{T}_H\tilde{V} - \tilde{\kappa}_I\rho\tilde{T}_H\tilde{I}_H + \tilde{\sigma}\tilde{I}_4 - \tilde{\mu}_I\tilde{I}_H, \tag{3.1d}$$

$$\frac{d\tilde{V}}{d\tau} = N\tilde{\mu}_I\tilde{I}_H - \tilde{\mu}_V\tilde{V}. \tag{3.1e}$$

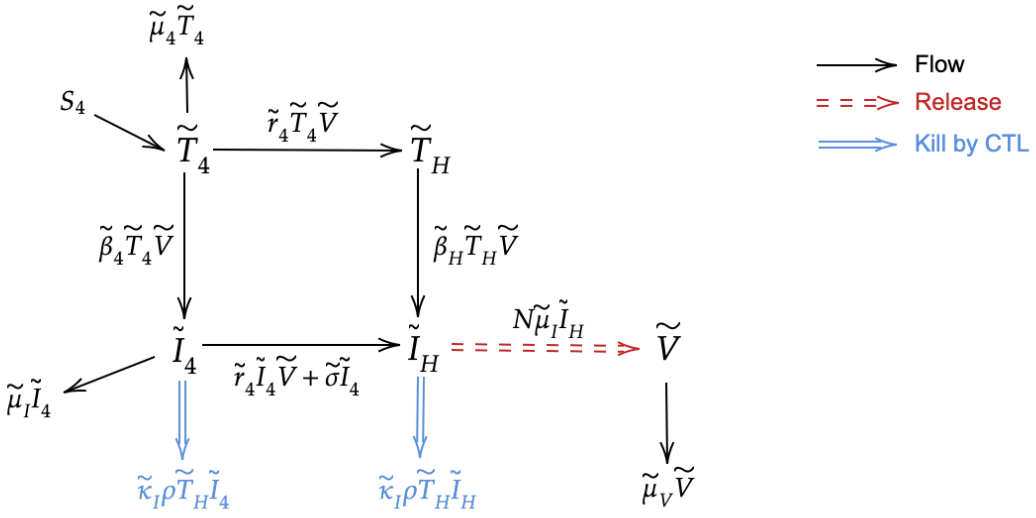


Figure 3.1: Progression diagram for the within-host HIV model with latent infections (model (3.1)).

To nondimensionalize the system (3.1), let $\tilde{T}_4 = S_4T_4/\tilde{\mu}_4$, $\tilde{T}_H = S_4T_H/\tilde{\mu}_4$, $\tilde{I}_4 = S_4I_4/\tilde{\mu}_4$, $\tilde{I}_H = S_4I_H/\tilde{\mu}_4$, $\tilde{V} = NS_4V/\tilde{\mu}_4$ and $\tau = t/\tilde{\mu}_V$. Then the non-dimensional parameters are $\kappa_I = \tilde{\kappa}_IS_4/(\tilde{\mu}_4\tilde{\mu}_V)$, $r_4 = \tilde{r}_4NS_4/(\tilde{\mu}_4\tilde{\mu}_V)$, $\beta_H = \tilde{\beta}_HNS_4/(\tilde{\mu}_4\tilde{\mu}_V)$, $\beta_4 = \tilde{\beta}_4NS_4/(\tilde{\mu}_4\tilde{\mu}_V)$, $\mu_I = \tilde{\mu}_I/\tilde{\mu}_V$, $\mu_4 = \tilde{\mu}_4/\tilde{\mu}_V$, $\mu_H = \tilde{\mu}_H/\tilde{\mu}_V$, $p_H = \tilde{p}_H/\tilde{\mu}_V$ and $\sigma = \tilde{\sigma}/\tilde{\mu}_V$. The nundimensional system is given below.

$$\frac{dT_4}{dt} = \mu_4 - \beta_4 T_4 V - r_4 T_4 V - \mu_4 T_4, \tag{3.2a}$$
$$\frac{dT_H}{dt} = r_4 T_4 V - \beta_H T_H V - d_H T_H, \tag{3.2b}$$
$$\frac{dI_4}{dt} = \beta_4 T_4 V - r_4 I_4 V - \kappa_I \rho T_H I_4 - \sigma I_4 - \mu_I I_4, \tag{3.2c}$$
$$\frac{dI_H}{dt} = r_4 I_4 V + \beta_H T_H V - \kappa_I \rho T_H I_H + \sigma I_4 - \mu_I I_H, \tag{3.2d}$$
$$\frac{dV}{dt} = \mu_I I_H - V. \tag{3.2e}$$

## 3.2 Disease-free Equilibrium

Model (3.2) has a disease-free equilibrium $(T_4^0, T_H^0, I_4^0, I_H^0, V) = (1, 0, 0, 0, 0)$. To compute the basic reproduction number $\mathcal{R}_0$, there are 4 disease compartments which are $T_H$, $I_4$, $I_H$ and $V$, and 1 non-disease compartment $T_4$ in model (3.2). Let $x = (x_1, x_2, x_3, x_4)^\top = (T_H, I_4, I_H, V)^\top$ and $f_i = dx_i/dt$. When $\mathcal{F}$ and $\mathcal{W}$ denote the inflow of secondary infections and progression of infections respectively,

$$\mathcal{F} = \begin{pmatrix} r_4 T_4 V \\ \beta_4 T_4 V \\ 0 \\ 0 \end{pmatrix}, \mathcal{W} = \begin{pmatrix} \beta_H T_H V + d_H T_H \\ r_4 I_4 V + \kappa_I \rho T_H I_4 + \sigma I_4 + \mu_I I_4 \\ -\beta_H T_H V - r_4 I_4 V + \kappa_I \rho T_H I_H - \sigma I_4 + \mu_I I_H \\ -\mu_I I_H + V \end{pmatrix}.$$

It is easy to prove that $\mathcal{F}$ and $\mathcal{W}$ satisfies the assumption A1-A5 in [24]. Let $F$ and $W$ be the $4 \times 4$ matrices with $ij$ entry equal to $F_{ij} = \frac{\partial \mathcal{F}_i}{\partial x_j}$ and $W_{ij} = \frac{\partial \mathcal{W}_i}{\partial x_j}$, evaluated at the disease-free equilibrium. According to [24], the basic reproduction number $\mathcal{R}_0$ is the spectral radius of the next generation matrix $FW^{-1}$, where

$$F = \begin{pmatrix} 0 & 0 & 0 & r_4 \\ 0 & 0 & 0 & \beta_4 \\ 0 & 0 & 0 & 0 \\ 0 & 0 & 0 & 0 \end{pmatrix}, W = \begin{pmatrix} d_H & 0 & 0 & 0 \\ 0 & \mu_I + \sigma & 0 & 0 \\ 0 & -\sigma & \mu_I & 0 \\ 0 & 0 & -\mu_I & 1 \end{pmatrix},$$

and

$$W^{-1} = \begin{pmatrix} \frac{1}{d_H} & 0 & 0 & 0 \\ 0 & \frac{1}{\mu_I+\sigma} & 0 & 0 \\ 0 & \frac{\sigma}{\mu_I(\mu_I+\sigma)} & \frac{1}{\mu_I} & 0 \\ 0 & \frac{\sigma}{\mu_I+\sigma} & 1 & 1 \end{pmatrix}.$$

Then,

$$FW^{-1} = \begin{pmatrix} 0 & \frac{r_4\sigma}{\mu_I+\sigma} & r_4 & r_4 \\ 0 & \frac{\beta_4\sigma}{\mu_I+\sigma} & \beta_4 & \beta_4 \\ 0 & 0 & 0 & 0 \\ 0 & 0 & 0 & 0 \end{pmatrix}.$$

Thus,

$$\mathcal{R}_0 = \rho(FW^{-1}) = \frac{\beta_4\sigma}{\mu_I+\sigma} = \frac{\tilde{\beta}_4 N S_4 \tilde{\sigma}}{\tilde{\mu}_4\tilde{\mu}_V(\tilde{\mu}_I+\tilde{\sigma})}. \tag{3.3}$$

To interpret $\mathcal{R}_0$, a single healthy naive CD4 T cell is infected at rate $\tilde{\beta}_4 S_4/\tilde{\mu}_4$ in a population of $\tilde{T}_4^0 = S_4/\tilde{\mu}_4$, and $\tilde{\sigma}/(\tilde{\mu}_I+\tilde{\sigma})$ gives the probability that infected cells progress from $\tilde{I}_4$ to $\tilde{I}_H$. The ratio $N/\tilde{\mu}_V$ is the average virus produced by an infected cell during its viral lifespan $1/\tilde{\mu}_V$. Linearization of the model (3.2) at the disease-free equilibrium gives Jacobian equal to $F-W$. If $\mathcal{R}_0 < 1$, all eigenvalues of $F-W$ have negative real part, then the disease-free equilibrium is locally asymptotically stable [24].

## 3.3 Endemic Equilibrium

To find the endemic equilibrium, let the right hand side of the system (3.2) equal zero. The endemic equilibrium of the 5-dimensional model for $T_4$, $T_H$, $I_4$ and $V$ is

$$\begin{aligned} T_4^* &= \frac{\mu_4}{(r_4+\beta_4)V^*+\mu_4}, && \text{(3.4a)} \\ T_H^* &= \frac{r_4 T_4^* V^*}{\beta_H V^* + d_H} = \frac{r_4\mu_4 V^*}{[(r_4+\beta_4)V^*+\mu_4][\beta_H V^* + d_H]}, && \text{(3.4b)} \\ I_4^* &= \frac{\beta_4 T_4^* V^*}{\mu_I + r_4 V^* + \kappa_I \rho T_H^* + \sigma}, && \text{(3.4c)} \\ V^* &= \mu_I I_H^*, && \text{(3.4d)} \end{aligned}$$

where

$$I_H^* = \frac{r_4 I_4^* V^* + \beta_H T_H^* V^* + \sigma I_4^*}{\mu_I + \kappa_I \rho T_H^*}. \tag{3.5}$$

We substitute the equation (3.4c) into the equation (3.5), then multiply by $[\mu_I + r_4 V^* + \kappa_I \rho T_H^* + \sigma][\mu_I + \kappa_I \rho T_H^*]$, giving

$$\begin{aligned} & \mu_I(\mu_I + r_4 V^* + \sigma) + (2\mu_I + r_4 V^* + \sigma)\kappa_I \rho T_H^* + (\kappa_I \rho T_H^*)^2 \\ = \;& \mu_I \left[\beta_4(r_4 V^* + \sigma)T_4^* + \beta_H \kappa_I \rho T_H^{*2} + \beta_H(\mu_I + r_4 V^* + \sigma)T_H^*\right]. \end{aligned}$$

Substituting $T_H^*$ into the equation above, and multiplying by $[(r_4+\beta_4)V^*+\mu_4]^2[\beta_H V^* + d_H]^2$ on both sides, gives the 5th degree polynomial

$$AV^{*5} + BV^{*4} + CV^{*3} + DV^{*2} + EV^* + G = 0, \tag{3.6}$$

where

$$
\begin{aligned}
A &= \mu_I r_4 \beta_H^2 (r_4+\beta_4)^2 > 0, && \text{(3.7a)}\\
B &= \mu_4 r_4^2 \kappa_I \rho \beta_H (r_4+\beta_4) + \mu_I(\mu_I+\sigma)(r_4+\beta_4)^2\beta_H^2 \\
&\quad +2\mu_I r_4 \beta_H[(r_4+\beta_4)^2 d_H + \mu_4\beta_H(r_4+\beta_4)] - \mu_I\mu_4 r_4 \beta_H^2 (r_4+\beta_4)^2, && \text{(3.7b)}\\
C &= \mu_4 r_4 \kappa_I \rho[r_4(r_4+\beta_4)d_H + \mu_4 r_4\beta_H + (2\mu_I+\sigma)(r_4+\beta_4)\beta_H] \\
&\quad +\mu_I r_4[(r_4+\beta_4)^2 d_H^2 + 4\mu_4\beta_H(r_4+\beta_4)d_H + \mu_4^2\beta_H^2] \\
&\quad +\mu_I(\mu_I+\sigma)[2\beta_H(r_4+\beta_4)^2 d_H + 2\mu_4\beta_H^2(r_4+\beta_4)] \\
&\quad -\mu_I\mu_4\beta_4[2r_4(r_4+\beta_4)\beta_H d_H + r_4\mu_4\beta_H^2] - \mu_I\mu_4\beta_4\sigma(r_4+\beta_4)\beta_H^2 \\
&\quad -\mu_I\mu_4 r_4\beta_H[r_4(r_4+\beta_4)d_H + \mu_4 r_4\beta_H + (r_4+\beta_4)\beta_H(\mu_I+\sigma)], && \text{(3.7c)}\\
D &= (\mu_4 r_4\kappa_I\rho)^2 + \mu_4 r_4\kappa_I\rho[\mu_4 r_4 d_H + (2\mu_I+\sigma)(r_4+\beta_4)d_H + (2\mu_I+\sigma)\mu_4\beta_H] \\
&\quad +\mu_I r_4[2\mu_4(r_4+\beta_4)d_H^2 + 2\mu_4^2\beta_H d_H] \\
&\quad +\mu_I(\mu_I+\sigma)[(r_4+\beta_4)^2 d_H^2 + 4\mu_4(r_4+\beta_4)\beta_H d_H + \mu_4^2\beta_H^2] \\
&\quad -\mu_I\mu_4 r_4\beta_4[(r_4+\beta_4)d_H^2 + 2\mu_4\beta_H d_H] - \mu_I\mu_4\beta_4\sigma[2(r_4+\beta_4)\beta_H d_H + \mu_4\beta_H^2] \\
&\quad -\mu_I\mu_4^2 r_4^2\beta_H\kappa_I\rho - \mu_I\mu_4 r_4\beta_H[\mu_4 r_4 d_H + (\mu_I+\sigma)(r_4+\beta_4)d_H \\
&\quad +(\mu_I+\sigma)\mu_4\beta_H], && \text{(3.7d)}\\
E &= \mu_4^2 r_4\kappa_I\rho(2\mu_I+\sigma)d_H + \mu_I\mu_4^2 r_4 d_H^2 + \mu_I(\mu_I+\sigma)[2\mu_4(r_4+\beta_4)d_H^2 + 2\mu_4^2\beta_H d_H] \\
&\quad -\mu_I\mu_4^2 r_4\beta_4 d_H^2 - \mu_I\mu_4\beta_4\sigma[(r_4+\beta_4)d_H^2 + 2\mu_4\beta_H d_H] \\
&\quad -\mu_I\mu_4^2 r_4\beta_H(\mu_I+\sigma)d_H, && \text{(3.7e)}\\
G &= \mu_I\mu_4^2 d_H^2[\mu_I + (1-\beta_4)\sigma]. && \text{(3.7f)}
\end{aligned}
$$

From the $\mathcal{R}_0$ (equation (3.3)), if $\mathcal{R}_0 > 1$, $G < 0$. The 5th degree order polynomial equation (3.6) has one, three or five positive roots. When $\mathcal{R}_0 > 1$, numerical simulations indicate that the system (3.2) has only one positive equilibrium.

## 3.4 Backward Bifurcation

Let

$$a = c^2\left[-\frac{(r_4+\beta_4)\beta_4}{\mu_4} - \frac{r_4}{\sigma} - \frac{r_4\kappa_I\rho}{d_H\sigma} + \frac{r_4\beta_4}{\sigma} + \frac{r_4\beta_4\beta_H}{d_H} - \frac{r_4\beta_4\kappa_I\rho}{\mu_I d_H}\right], \quad (3.8a)$$

$$b = c > 0, \quad (3.8b)$$

be the coefficient of backward bifurcation, where

$$c = \frac{1}{1/\sigma + \beta_4/\mu_I + \beta_4}$$

and

$$\beta_4 = 1 + \mu_I/\sigma.$$

We derive the $a$ and $b$ in the proof of Theorem 2. Note that signs of $a$ and $b$ determine the type and direction of bifurcation.

**Theorem 2.** *Consider the within-host HIV model defined by (3.2) with a defined in (3.8). Then*

- *if $a > 0$, there exists a backward bifurcation at $\mathcal{R}_0 = 1$;*
- *if $a < 0$, there exists a forward bifurcation at $\mathcal{R}_0 = 1$.*

*Proof.* Let $x = (x_1, x_2, x_3, x_4, x_5)^\top = (T_4, T_H, I_4, I_H, V)^\top$ and $f_i = dx_i/dt$ from the model (3.2). Since $E^0 = (T_4^0, T_H^0, I_4^0, I_H^0, V^0) = (1, 0, 0, 0, 0)$ is the disease-free equilibrium always, the linearization of the system (3.2) at the disease-free equilibrium is

$$J = \begin{pmatrix} -\mu_4 & 0 & 0 & 0 & -(r_4+\beta_4) \\ 0 & -d_H & 0 & 0 & r_4 \\ 0 & 0 & -\mu_I - \sigma & 0 & \beta_4 \\ 0 & 0 & \sigma & -\mu_I & 0 \\ 0 & 0 & 0 & \mu_I & -1 \end{pmatrix}. \quad (3.9)$$

When the Jacobian matrix (3.9) has an eigenvalue zero, equivalently $\mathcal{R}_0 = 1$ and

$$\beta_4 = 1 + \mu_I/\sigma,$$

the corresponding left eigenvector $\mathbf{v}^\top$ and right eigenvector $\mathbf{w}$ at eigenvalue zero are

$$\mathbf{v} = \begin{pmatrix} 0 \\ 0 \\ 1 \\ \beta_4 \\ \beta_4 \end{pmatrix}, \ \mathbf{w} = c \begin{pmatrix} -(r_4+\beta_4)/\mu_4 \\ r_4/d_H \\ 1/\sigma \\ 1/\mu_I \\ 1 \end{pmatrix},$$

where $c = \frac{1}{1/\sigma+\beta_4/\mu_I+\beta_4} = \frac{\mu_I\sigma}{2\mu_I+\mu_I^2+\sigma}$.

Let $\beta_4$ be the bifurcation parameter. The nonzero second order derivatives used to compute $b$ at $\mathcal{R}_0 = 1$ (i.e. $\beta_4 = 1 + \mu_I/\sigma$) are

$$\frac{\partial^2 f_3}{\partial x_5 \partial \mathcal{R}_0}(E^0, (\sigma+\mu_I)/\sigma) \ = \ 1.$$

Thus,

$$b = \sum_{i,j=1}^{5} v_i w_j \frac{\partial^2 f_i}{\partial x_j \partial \mathcal{R}_0}(E^0, 1) = v_3 w_5 \frac{\partial^2 f_3}{\partial x_5 \partial \mathcal{R}_0}(E^0, (\sigma+\mu_I)/\sigma) = c > 0.$$

The nonzero second order derivatives used to compute $a$ at $\mathcal{R}_0 = 1$ are

$$\begin{aligned}
\frac{\partial^2 f_3}{\partial x_1 \partial x_5}(E^0, (\sigma+\mu_I)/\sigma) &= 1 + \mu_I/\sigma, \\
\frac{\partial^2 f_3}{\partial x_3 \partial x_5}(E^0, (\sigma+\mu_I)/\sigma) &= -r_4, \\
\frac{\partial^2 f_3}{\partial x_2 \partial x_3}(E^0, (\sigma+\mu_I)/\sigma) &= -\kappa_I \rho, \\
\frac{\partial^2 f_4}{\partial x_3 \partial x_5}(E^0, (\sigma+\mu_I)/\sigma) &= r_4, \\
\frac{\partial^2 f_4}{\partial x_2 \partial x_5}(E^0, (\sigma+\mu_I)/\sigma) &= \beta_H, \\
\frac{\partial^2 f_4}{\partial x_2 \partial x_4}(E^0, (\sigma+\mu_I)/\sigma) &= -\kappa_I \rho.
\end{aligned}$$

Thus,

$$\begin{aligned}
a &= \sum_{i,j,k=1}^{5} v_i w_j w_k \frac{\partial^2 f_i}{\partial x_j \partial x_k}(E^0, 1) \\
&= v_3 w_1 w_5 \frac{\partial^2 f_3}{\partial x_1 \partial x_5}(E^0, (\sigma+\mu_I)/\sigma) + v_3 w_3 w_5 \frac{\partial^2 f_3}{\partial x_3 \partial x_5}(E^0, (\sigma+\mu_I)/\sigma) \\
&\quad + v_3 w_2 w_3 \frac{\partial^2 f_3}{\partial x_2 \partial x_3}(E^0, (\sigma+\mu_I)/\sigma) + v_4 w_3 w_5 \frac{\partial^2 f_4}{\partial x_3 \partial x_5}(E^0, (\sigma+\mu_I)/\sigma) \\
&\quad + v_4 w_2 w_5 \frac{\partial^2 f_4}{\partial x_2 \partial x_5}(E^0, (\sigma+\mu_I)/\sigma) + v_4 w_2 w_4 \frac{\partial^2 f_4}{\partial x_2 \partial x_4}(E^0, (\sigma+\mu_I)/\sigma) \\
&= c^2 \left[ -\frac{(r_4+\beta_4)\beta_4}{\mu_4} - \frac{r_4}{\sigma} - \frac{r_4 \kappa_I \rho}{d_H \sigma} + \frac{r_4 \beta_4}{\sigma} + \frac{r_4 \beta_4 \beta_H}{d_H} - \frac{r_4 \beta_4 \kappa_I \rho}{\mu_I d_H} \right] \\
&= c^2 \left[ -\frac{(r_4+1+\mu_I/\sigma)(1+\mu_I/\sigma)}{\mu_4} - \frac{r_4}{\sigma} - \frac{r_4 \kappa_I \rho}{d_H \sigma} + \frac{r_4(1+\mu_I/\sigma)}{\sigma} \right. \\
&\quad \left. + \frac{r_4(1+\mu_I/\sigma)\beta_H}{d_H} - \frac{r_4(1+\mu_I/\sigma)\kappa_I \rho}{\mu_I d_H} \right].
\end{aligned}$$

□

According to the equation (3.8), increasing the value of $\beta_H$ results in the larger number of $a$, making the backward bifurcation easier to happen. Moreover, decreasing the value of $\rho$ also makes the backward bifurcation more likely.

**Remark 2.** *Note that*

$$a = -\frac{1}{(1/\sigma + \beta_4/\mu_I + \beta_4)^2 \mu_I \sigma} E.$$

*Thus, $a > 0$ if and only if $E < 0$. The backward bifurcation condition is equivalent to $E < 0$.*

*Proof.* From the equation (3.8), and setting $\mathcal{R}_0 = 1$, i.e, $\beta_4 = 1 + \mu_I/\sigma$,

$$\begin{aligned}
a &= c^2 \left[ -\frac{(r_4+\beta_4)\beta_4}{\mu_4} - \frac{r_4}{\sigma} - \frac{r_4 \kappa_I \rho}{d_H \sigma} + \frac{r_4 \beta_4}{\sigma} + \frac{r_4 \beta_4 \beta_H}{d_H} - \frac{r_4 \beta_4 \kappa_I \rho}{\mu_I d_H} \right] \\
&= \frac{c^2}{\mu_I \mu_4 d_H \sigma^2} \left[ \mu_I^2 \mu_4 r_4 d_H + \mu_I \mu_4 r_4 \beta_H \sigma^2 + \mu_I^2 \mu_4 r_4 \beta_H \sigma - \mu_I (r_4+1) d_H \sigma^2 \right. \\
&\quad \left. - \mu_I^2 (r_4+1) d_H \sigma - \mu_I^2 d_H \sigma - \mu_I^3 d_H - 2\mu_I \mu_4 r_4 \kappa_I \rho \sigma - \mu_4 r_4 \kappa_I \rho \sigma^2 \right].
\end{aligned}$$

If $a > 0$,

$$\mu_I(r_4+1)d_H\sigma^2 + \mu_I^2(r_4+1)d_H\sigma + \mu_I^2 d_H\sigma + \mu_I^3 d_H + 2\mu_I\mu_4 r_4\kappa_I\rho\sigma + \mu_4 r_4\kappa_I\rho\sigma^2$$
$$< \mu_I^2\mu_4 r_4 d_H + \mu_I\mu_4 r_4\beta_H\sigma^2 + \mu_I^2\mu_4 r_4\beta_H\sigma.$$

From the equation (3.7a),

$$\begin{aligned} E &= \mu_4^2 r_4\kappa_I\rho(2\mu_I+\sigma)d_H + \mu_I\mu_4^2 r_4 d_H^2(1-\beta_4) + \mu_I(\mu_I+\sigma)\left[2\mu_4(r_4+\beta_4)d_H^2\right. \\ &\quad \left.+2\mu_4^2\beta_H d_H\right] - \mu_I\mu_4\beta_4\sigma[(r_4+\beta_4)d_H^2 + 2\mu_4\beta_H d_H] - \mu_I\mu_4^2 r_4\beta_H(\mu_I+\sigma)d_H \\ &= \frac{\mu_4 d_H}{\sigma}\left[2\mu_I\mu_4 r_4\kappa_I\rho\sigma + \mu_4 r_4\kappa_I\rho\sigma^2 + \mu_I^2(1+r_4)d_H\sigma + \mu_I^3 d_H + \mu_I(1+r_4)d_H\sigma^2\right. \\ &\quad \left.+\mu_I^2 d_H\sigma - \mu_I^2\mu_4 r_4 d_H - \mu_I^2\mu_4 r_4\beta_H\sigma - \mu_I\mu_4 r_4\beta_H\sigma^2\right]. \end{aligned}$$

Thus, if $a > 0$, $E < 0$ and vice versa. □

Because $\mathcal{R}_0$ depends on the value of $\beta_4$, we changed $\beta_4$ to change $\mathcal{R}_0$. To simulate the model (3.2), we firstly obtained the positive equilibria for different $\mathcal{R}_0$ by solving the root of the 5th degree polynomial (3.6). The dimensional parameter values $S_4$, $N$, $\tilde{\mu}_4$, $\tilde{\mu}_I$, $\tilde{\mu}_V$, $\tilde{\mu}_H$, $\tilde{p_H}$ and $\tilde{\kappa}_I$ are from the Hogue et al. model [9]. We set $\tilde{\beta}_H = 2\times10^{-9}$. Figure 3.2 demonstrates the endemic equilibria for different values of $\rho$. Moreover, we checked the stability of endemic equilibria numerically by evaluating the Jacobian. In Figure 3.2a and 3.2b, the lower branch with the red dashed line denotes the unstable endemic equilibrium while the higher branch with the black solid line is a locally asymptotically stable endemic equilibrium.

In Figure 3.2a, we pick $\rho = 1.1525$, the corresponding backward bifurcation coefficient $a > 0$ at $\mathcal{R}_0 = 1$, indicating that there exists a backward bifurcation when $\mathcal{R}_0 < 1$. However, the critical value $\mathcal{R}_C$ is negative, which means there are two endemic equilibria coexisting when $\mathcal{R}_0 < 1$ and $\rho$ is small enough. Then we increase the $\rho$ value from 1.1525 to 1.1575 in Figure 3.2b, giving a positive critical value $\mathcal{R}_C$. The corresponding bifurcation coefficient $a > 0$, which confirms the fact that there exists a backward bifurcation. With these parameter values, decreasing the value of $\mathcal{R}_0$ with drug therapy might drive HIV to the disease-free equilibrium. In Figure 3.2c,

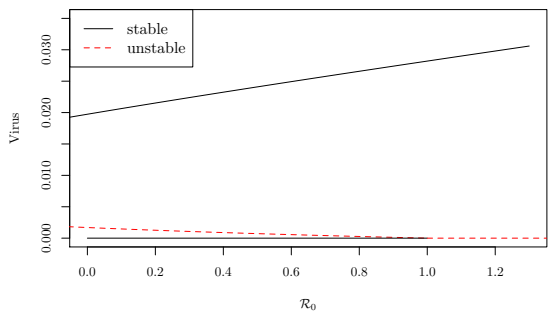


(a) Bistability when $\rho = 1.1525$

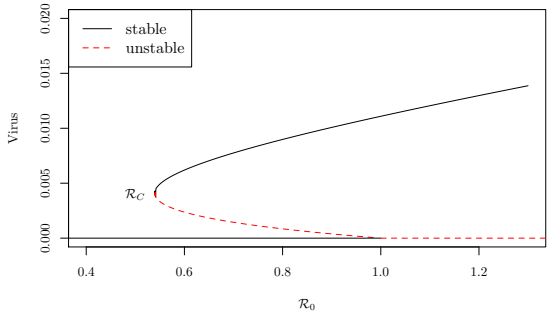


(b) Backward Bifurcation when $\rho = 1.1575$

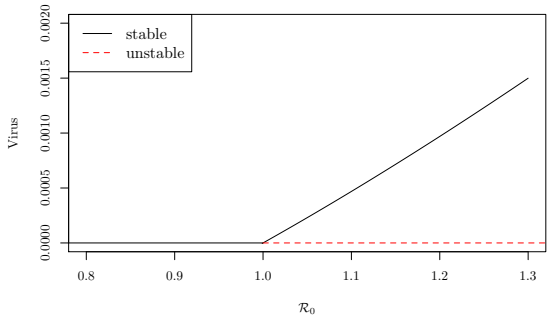


(c) Forward Bifurcation when $\rho = 1.1625$

Figure 3.2: The bifurcation diagram of the equilibrium viral load for model (3.2), using $\mathcal{R}_0$ as the bifurcation parameter. Here $\mu_4 = 3.875$, $\beta_H = 525$, $r_4 = 525$, $\kappa_I = 1750$, $\mu_I = 3.875$, $\mu_H = 3.875$, $p_H = 1.5$, $\sigma = 5250$. Parameter values except $\sigma$ come from Hogue et al. model [9].

there exists a forward bifurcation and a unique endemic equilibrium. This result is explained by the fact that when the value of $\rho$ is large enough, the coefficient $a$ is negative and the backward bifurcation condition is not satisfied.

Mathematically, the bistability means the coexistence of a locally stable disease-free equilibrium and a locally stable endemic equilibrium. Figures 3.2a and 3.2b show that, for $\mathcal{R}_0 < 1$, the outcome of the infection is initial value dependent. A small initial value would drive the total viral load to the disease-free equilibrium. With a large initial value or an initial condition adjacent to the locally asymptotically stable

endemic equilibrium, HIV will persist.

## 3.5 Concluding Remarks

In this chapter, we create a model that contains the latent infection of naive CD4 T cells to illustrate the viral dynamics in the acute stage. This model still exhibits bistability. When the helper T cells and activation of latent infection are not present, i.e, $r_4 = 0$, the backward bifurcation does not exist. In general, when $\rho$ is proportion to the load of CTLs, the level of CTLs determines the existence of backward bifurcation (i.e, large $\rho$ prevent the existence of backward bifurcation). Small values of the killing rate of CTLs $\kappa_I$ and large values of the infection rate for T helper cells $\beta_H$ promote the backward bifurcation in the model (2.3) and model (3.2). In our 5-dimension model (3.2), the long-lived latent reservoir is not included because we do not consider the effect of drug treatment.

The killing rate of latent infected CD4 T cells and T helper cells by CTL may be different, and the latent infected cells may not be killed by the immune response [22, page 2]. Thus a future model should distinguish these two killing terms.

# Chapter 4

# Viral Diversity and Progression to AIDS

There are some factors that result in HIV genetic variation: low replication accuracy during reverse transcription (about 0.2 errors per genome for each replication cycle), recombination during reverse transcription and selective pressure [19, 14]. In the course of progression to AIDS, total viral load depends on viral growth rate, killing rate by the immune response system, and the antigenic diversity. Furthermore, HIV can destroy immune responses, which leads to viral load blows up. Based on these assumptions, Nowak and May [14] generate a simple model of antigenic variation, which is shown below,

$$\frac{dv_i}{dt} = rv_i - px_iv_i, \tag{4.1a}$$

$$\frac{dx_i}{dt} = cv_i - bx_i, \tag{4.1b}$$

where $v_i$ denotes the specific viral strain $i$, $x_i$ is the strain-specific immune response against viral strain $v_i$. The population size of $v_i$ grows at a rate $r$, strain-specific immune responses are stimulated by viral strain $v_i$ at a rate $c$. Viral strain $v_i$ is killed by $x_i$ at a rate $p$. The death rate of $x_i$ is $b$. Note that the new mutant viral strain grows initially before the immune responses against this new viral strain are evoked.

The model (4.1) shows that each viral strain has the same steady state, namely

$v_i^* = br/cp$, and the total viral load $v^* = \sum_{i=1}^{n} v_i^*$ increases linearly with an increasing number of viral strains. The same is true for the equilibrium immune response $x^*$. However it ignores the elimination of the immune system by the virus, which is the key feature of HIV. It is also unrealistic that each viral strain is independent of all the others. An extended model [14, 27] that contains the group-specific immune responses against all mutant viral strains is introduced.

In this chapter, we review the Wodarz and Nowak model [27] in Sections 4.1 and 4.2, and construct a model with carrying capacity in Section 4.3. We conclude that when the supply of target cells is limited, there does not exist a diversity threshold as in the Wodarz and Nowak model [27].

## 4.1 Review of Wodarz and Nowak Model

The model of Wodarz and Nowak [27] includes multiple viral strains $v_i$ for $i = 1, ..., n$, the strain-specific immune response against specific viral strains $x_i$ and the group-specific immune response against all type of viral strains $z$.

$$\frac{dv_i}{dt} = v_i(r - px_i - sz), \tag{4.2a}$$

$$\frac{dx_i}{dt} = kv_i - bx_i - uvx_i, \tag{4.2b}$$

$$\frac{dz}{dt} = k'v - bz - uvz, \tag{4.2c}$$

where $v = \sum_{i=1}^{n} v_i$ denotes the total viral load. This model does not consider the cross immunity between strains. All strain-specific immune responses $x_i$ are evoked by viral strains $v_i$ at the same rate $k$, and they have the same death rate $b$. Group-specific immune responses are evoked by total viral strains at a constant rate $k'$. Both strain-specific and group-specific immune responses are impaired by total viral strains at the same rate $u$. Also, to make this model simple, all viral strains are assumed to have the same replication rate $r$, and are killed at the rates $p$ and $s$ by strain-specific immune responses and group-specific immune responses respectively. The variables and parameters are summarized in Table 4.1.

| | |
|---|---|
| $x_i$ | the strain-specific immune response against viral strain $i$ |
| $v_i$ | viral strain $i$ |
| $z$ | the group-specific immune response against all types of viral strains |
| $r$ | the average rate of replication |
| $p$ | the efficacy of the strain-specific immune response |
| $s$ | the efficacy of the group-specific immune response |
| $k$ | activation rate of the strain-specific immune response |
| $b$ | the decay rate of the immune response |
| $u$ | the ability of the virus to impair immune response |
| $k'$ | activation rate of the group-specific immune response |

Table 4.1: Summary of parameters for model (4.2).

Wodarz and Nowak [27] assume that the dynamics of strain-specific immune responses $x_i$ and the group-specific immune response $z$ are on a faster time scale than the dynamics of $v_i$. Thus, at an equilibrium,

$$x_i^* = \frac{kv_i}{b+uv},$$
$$z^* = \frac{k'v}{b+uv}.$$

Then the total viral load changes with time as

$$\frac{dv}{dt} = \sum_{i=1}^{n} \frac{dv_i}{dt} = rv - \frac{pk\sum_{i=1}^{n} v_i^2}{b+uv} - \frac{sk'v^2}{b+uv}. \tag{4.3}$$

The viral diversity is measured by the Simpson index $D = \sum_{i=1}^{n}(v_i/v)^2$. Thus $\sum_{i=1}^{n} v_i^2 = v^2 D$, and equation (4.3) becomes

$$\frac{dv}{dt} = rv - \frac{pkv^2 D}{b+uv} - \frac{sk'v^2}{b+uv}. \tag{4.4}$$

Then the total viral load $v$ converges to a steady state

$$v^* = \frac{rb}{sk' + pkD - ru}. \tag{4.5}$$

In addition, $v_i^* = v^*/n$ and $D = 1/n$ at the steady state. Their model shows that the equilibrium of the total viral load depends on the number of viral strains. There are three situations derived from their model, the first one happens when the total viral load cannot be controlled by the immune responses, which is $ru > sk' + pk \geq sk' + pkD$. The second one arises when $k'/u > r/s$, which means the virus can be controlled by the group-specific responses and HIV does not progress to AIDS. The last situation happens when $sk' + pk > ru > sk'$, in this case, there is a threshold for the number of viral strains,

$$D^* = \frac{ru - sk'}{pk}.$$

When the viral diversity is below the threshold, the total viral load goes to an equilibrium. After $n$ increases beyond the threshold $1/D^*$, the total virus is unbounded. In this case, when the group-specific immune responses are not necessary to control the viral replication, i.e., $s = 0$, there still exists a threshold $D^* = ru/pk$. We demonstrate this in detail in Section 4.2.

The equilibrium strain-specific immune response

$$x^* = \sum_{i=1}^{n} x_i^* = \frac{kv^*}{b + uv^*}$$

is an increasing function of $v^*$. This model predicts that, when a patient develops AIDS, i.e., when $v^*$ approaches $\infty$, $x^*$ approaches its maximum. However, data suggest that the total CD4 T cell count decreases to zero with the development to AIDS [27].

Because their model does not consider the limited supply of CD4 T cells, in Section 4.3, we add carrying capacity for the virus and consider whether there still exists a threshold.

## 4.2 Wodarz and Nowak Model without Carrying Capacity

Firstly, we simplify the Wodarz and Nowak model [27] by ignoring the effect of group-specific immune responses. The $2n$-dimensional model without carrying capacity is shown below,

$$\frac{dv_i}{dt} = v_i(r - px_i), \tag{4.6a}$$

$$\frac{dx_i}{dt} = kv_i - bx_i - ux_i \sum_{i=1}^{n} v_i. \tag{4.6b}$$

The variables and parameters are the same as in equation (4.2) (see Table 4.1).

This model has a unique endemic equilibrium,

$$x_i^* = r/p, \tag{4.7a}$$

$$v_i^* = \frac{bx_i^* + ux_i^* \sum_{i=1}^{n} v_i^*}{k} = \frac{rb + ru \sum_{i=1}^{n} v_i^*}{pk}. \tag{4.7b}$$

The equilibrium values of $v_i^*$ are the same. Thus we can conclude that the equilibrium of total virual load is

$$V^* = \sum_{i=1}^{n} v_i^* = \frac{rb}{pk/n - ru}. \tag{4.8}$$

When $n$ goes to $pk/(ru)$, the total viral load goes to infinity. When $n < pk/(ru)$, the total viral load is bounded. The critical transition occurs when $n = \frac{pk}{ru}$. Once this threshold of viral diversity is exceeded, then the virus population escapes from control by the immune response and tends to arbitrarily high densities. This leads to AIDS. During the asymptomatic phase, the diversity is increasing, but the immune system is able to control viral densities and to maintain CD4 T cell levels.

The equilibrium immune response $x^* = \sum_{i=1}^{n} x_i^* = rn/p$, which increases linearly with viral diversity. Thus this model has the same limitation as model (4.2). In the next section, we incorporate the carrying capacity of viral load into model (4.6).

## 4.3 Wodarz and Nowak Model with Carrying Capacity

We modify model (4.6) by adding carrying capacity to the total viral load. We aim to analyze if the total virus increases with an increasing number of viral strains. The modified model is

$$\frac{dv_i}{dt} = (r - \frac{r}{M}v_i)v_i - pv_ix_i, \tag{4.9a}$$

$$\frac{dx_i}{dt} = kv_i - bx_i - ux_i\sum_{i=1}^{n} v_i, \tag{4.9b}$$

where the constant $M$ denotes the carrying capacity. To obtain the disease-free equilibrium and endemic equilibrium, we set the right hand side of the model (4.9) equals zero. The disease-free equilibrium $(x_i^0, v_i^0) = (0, 0)$ is unstable. The unique endemic equilibrium of the immune responses and virus are

$$x_i^* = \frac{kv_i^*}{b + u\sum_{i=1}^{n} v_i^*},$$

and

$$v_i^* = \frac{rM(b + u\sum_{i=1}^{n} v_i^*)}{r(b + u\sum_{i=1}^{n} v_i^*) + pkM},$$

when the viral load is positive. All viral strains have the same abundance at their equilibrium. Thus the total viral load at equilibrium is $V^* = \sum v_i^* = nv_i^*$

**Theorem 3.** *In the model (4.9), the total viral load at equilibrium increases faster with an increasing number of viral strains.*

*Proof.* We aim to find if $\frac{\partial V^*}{\partial n} > 0$ and $\frac{\partial^2 V^*}{\partial n^2} > 0$ when $\frac{\partial V^*}{\partial n}$ is the change rate of the equilibrium total viral load with respect to the number of viral strains. The endemic equilibrium of total viral load $V^*$ is the positive root of

$$V^{*2} - (nM - \frac{b}{u} - \frac{pkM}{ru})V^* - \frac{nbM}{u} = 0, \tag{4.10}$$

which is

$$V^* = \frac{1}{2}\left[nM - \frac{b}{u} - \frac{pkM}{ru} + \sqrt{\left(nM - \frac{b}{u} - \frac{pkM}{ru}\right)^2 + \frac{4nbM}{u}}\right]. \tag{4.11}$$

Then we take first derivative of equation (4.10) with respect to $n$:

$$2V^*\frac{\partial V^*}{\partial n} - (nM - \frac{b}{u} - \frac{pkM}{ru})\frac{\partial V^*}{\partial n} - MV^* - \frac{b}{u}M = 0, \tag{4.12}$$

then we obtain

$$\frac{\partial V^*}{\partial n} = \frac{MV^* + \frac{b}{u}M}{2V^* - nM + \frac{b}{u} + \frac{pkM}{ru}}.$$

We take the second derivative of equation (4.12) with respect to $n$:

$$2V^*\frac{\partial^2 V^*}{\partial n^2} + 2(\frac{\partial V^*}{\partial n})^2 - 2M\frac{\partial V^*}{\partial n} - (nM - \frac{b}{u} - \frac{pkM}{ru})\frac{\partial^2 V^*}{\partial n^2} = 0,$$

then we obtain

$$\frac{\partial^2 V^*}{\partial n^2} = \frac{2M\frac{\partial V^*}{\partial n} - 2(\frac{\partial V^*}{\partial n})^2}{2V^* - nM + \frac{b}{u} + \frac{pkM}{ru}}.$$

Next we aim to show the denominator of $\frac{\partial V^*}{\partial n}$ is positive. We substitute the equation (4.11) into the denominator of $\frac{\partial V^*}{\partial n}$, which is given

$$2V^* - nM + \frac{b}{u} + \frac{pkM}{ru} = \sqrt{\left(nM - \frac{b}{u} - \frac{pkM}{ru}\right)^2 + \frac{4nbM}{u}} > 0. \tag{4.13}$$

Then the denominators of $\frac{\partial V^*}{\partial n}$ and $\frac{\partial^2 V^*}{\partial n^2}$ are positive, and

$$\frac{\partial V^*}{\partial n} > 0.$$

We aim to check if the numerator of $\frac{\partial^2 V^*}{\partial n^2}$ is positive, because

$$M - \frac{\partial V^*}{\partial n} = \frac{M[V^* - nM + pkM/ru]}{2V^* - nM + b/u + pkM/ru}, \tag{4.14}$$

where

$$V^* - nM + \frac{pkM}{ru} = \frac{1}{2}\left[-nM - \frac{b}{u} + \frac{pkM}{ru} + \sqrt{\left(nM - \frac{b}{u} - \frac{pkM}{ru}\right)^2 + \frac{4nbM}{u}}\right]. \tag{4.15}$$

Because

$$\begin{aligned}\sqrt{\left(nM-\frac{b}{u}-\frac{pkM}{ru}\right)^2+\frac{4nbM}{u}} &> \left|nM-\frac{b}{u}-\frac{pkM}{ru}\right| \\ &\geq -nM+\frac{b}{u}+\frac{pkM}{ru} \\ &> -nM-\frac{b}{u}+\frac{pkM}{ru},\end{aligned}$$

it follows that $V^*-nM+pkM/ru>0$, which implies

$$M>\frac{\partial V^*}{\partial n} \quad \text{and} \quad \frac{\partial^2 V^*}{\partial n^2}>0.$$

□

Here $\frac{\partial V^*}{\partial n}>0$ implies that the viral load $V$ is an increasing function of the number of viral strains $n$, and $\frac{\partial^2 V^*}{\partial n^2}>0$ illustrates that the viral load grows faster with increasing viral diversity. Because the equilibrium strain-specific immune responses $x_i^*$ are identical, the total equilibrium immune response is

$$x^*=\sum_{i=1}^{n}x_i^*=nx_i^*=\frac{kV^*}{b+uV^*}. \tag{4.16}$$

The viral diversity results in the growth of immune responses since $\frac{\partial x^*}{\partial n}=\frac{\partial x^*}{\partial V^*}\frac{\partial V^*}{\partial n}$, and each partial derivative is positive, which means that the immune response is an increasing function of the viral diversity. As is the case for models (4.2) and (4.6), this model does not capture the observed CD4 T cell dynamics in HIV.

## 4.4 Concluding Remarks

In this chapter, we simplified the Wodarz and Nowak model [27], mainly ignoring the group-specific immune response. We showed that this is not crucial for the existence of a threshold of viral diversity. Models (4.2), (4.6) and (4.9) give the same result: the growth of total viral load depends on the viral mutation and antigenic variation, and viral evolution might drive the progression to AIDS. Furthermore, the model (4.6) and the model (4.9) illustrate that each mutant viral strain has the same abundance at

their steady state. There exists a diversity threshold in the Wodarz and Nowak model (4.2) and the model (4.6) when the supply of healthy naive CD4 T cells is unlimited. However the diversity threshold does not exist in the model (4.9), which is more realistic, when it includes the carrying capacity on the viral load. The population size of the virus always goes to a steady-state, and the endemic equilibrium of the virus increases with an increasing number of viral strains. However, these models predict that the equilibrium immune response increases with viral diversity. In the next chapter, we incorporate viral diversity into model (2.3), to investigate if a model with more realistic HIV dynamics shows the same feature for the viral load dynamics, but has a realistic immune response dynamics.

It may be more reasonable to assume a carrying capacity for the total viral load rather than each specific strain, i.e., it is better to use $r[1-(v_1+\ldots+v_n)/M]v_i$ for the viral reproduction. This is a direction for future research, the viral load may not be concave up.

# Chapter 5

# Within-host HIV Model with Viral Strains

In Chapter 2, we studied a simple within-host HIV model (2.3) that captures the key features of HIV dynamics. In Chapter 4, we demonstrated that viral evolution enlarges the total viral load. In this chapter, we add viral strains to the non-dimensional model (2.3) to analyze how viral evolution influences the total viral load, T helper cells and naive CD4 T cells.

## 5.1 Within-host HIV Model with Viral Diversity

We let $V_i$ denote the viral strain $i$. We assume that naive CD4 T cells are infected by the total viral load $\sum_{i=1}^{n} V_i$ at a rate $\beta_4 T_4 \sum_{i=1}^{n} V_i$, and are produced at a constant rate $\mu_4$. Viral strain $V_i$ can activate CD4 T cells to become strain-specific helper T cells $T_{Hi}$ at a rate $r_4 T_4 V_i$. As the second susceptible class, $T_{Hi}$ can be infected by the total viral load at a rate $\beta_H T_{Hi} \sum_{i=1}^{n} V_i$. When T helper cells and naive CD4 T cells are infected by the strain-specific virus $V_i$, we denote the strain-specific infected cells by $I_i$. Each strain-specific T helper cell has the identical natural death rate $\mu_H$ and proliferation rate $p_H$. Moreover, each strain-specific infected cell dies from the infection at a constant rate $\mu_I$, and is killed by the immune system at a rate $\kappa_I T_{Hi}$.

The modified model is given below,

$$\frac{dT_4}{dt} = \mu_4 - r_4 T_4 \sum_{i=1}^{n} V_i - \beta_4 T_4 \sum_{i=1}^{n} V_i - \mu_4 T_4, \tag{5.1a}$$

$$\frac{dT_{Hi}}{dt} = r_4 T_4 V_i - \beta_H T_{Hi} \sum_{i=1}^{n} V_i - \mu_H T_{Hi} + p_H T_{Hi}, \tag{5.1b}$$

$$\frac{dI_i}{dt} = \beta_H V_i \sum_{i=1}^{n} T_{Hi} + \beta_4 T_4 V_i - \mu_I I_i - \kappa_I \rho T_{Hi} I_i, \tag{5.1c}$$

$$\frac{dV_i}{dt} = \mu_I I_i - V_i. \tag{5.1d}$$

If we let the total T helper cells be denoted by $T_H = \sum_{i=1}^{n} T_{Hi}$, the above model becomes

$$\frac{dT_4}{dt} = \mu_4 - r_4 T_4 \sum_{i=1}^{n} V_i - \beta_4 T_4 \sum_{i=1}^{n} V_i - \mu_4 T_4, \tag{5.2a}$$

$$\frac{dT_H}{dt} = r_4 T_4 \sum_{i=1}^{n} V_i - \beta_H T_H \sum_{i=1}^{n} V_i - \mu_H T_H + p_H T_H, \tag{5.2b}$$

$$\frac{dI_i}{dt} = \beta_H T_H V_i + \beta_4 T_4 V_i - \mu_I I_i - \kappa_I \rho T_{Hi} I_i, \tag{5.2c}$$

$$\frac{dV_i}{dt} = \mu_I I_i - V_i. \tag{5.2d}$$

## 5.2 Endemic Equilibrium Depends on Viral Strains

By setting the right hand side in model (5.2) equal to zero, the endemic equilibrium values of $T_4^*$, $T_H^*$, $T_{Hi}^*$ and $I_i^*$ in terms of $V_i^*$ are

$$T_4^* = \frac{\mu_4}{\mu_4 + (r_4 + \beta_4) \sum_{i=1}^{n} V_i^*}, \tag{5.3a}$$

$$T_H^* = \frac{r_4 T_4^* \sum_{i=1}^{n} V_i^*}{\beta_H \sum_{i=1}^{n} V_i^* + \mu_H - p_H}, \tag{5.3b}$$

$$T_{Hi}^* = \frac{r_4 T_4^* V_i^*}{\beta_H \sum_{i=1}^{n} V_i^* + \mu_H - p_H}, \tag{5.3c}$$

$$I_i^* = \frac{V_i^*}{\mu_I}, \tag{5.3d}$$

and the equilibrium viral load $V_i^*$ satisfies

$$\beta_H V_i^* \sum_{i=1}^{n} T_{Hi}^* + \beta_4 T_4^* V_i^* - \mu_I I_i^* - \kappa_I \rho T_{Hi}^* I_i^* = 0. \tag{5.4}$$

We plug $T_H^*$ and $T_{Hi}^*$ into equation (5.4) and let the total viral load at the steady state be $L = \sum_{i=1}^{n} V_i^*$, then equation (5.4) simplified gives,

$$\frac{\beta_H r_4 T_4^* L}{\beta_H L + d_H} + \beta_4 T_4^* - 1 - \frac{\kappa_I \rho r_4 T_4^* V_i^*}{\mu_I(\beta_H L + d_H)} = 0. \tag{5.5}$$

Then multiplying by $\mu_I(\beta_H L + d_H)$, equation (5.5) becomes

$$\beta_H \mu_I r_4 T_4^* L + \beta_4 \mu_I T_4^* (\beta_H L + d_H) - (\beta_H L + d_H)\mu_I - \kappa_I \rho r_4 T_4^* V_i^* = 0. \tag{5.6}$$

Then substituting $T_4^*$ in equation (5.6), gives

$$\beta_H \mu_I \mu_4 r_4 L + \beta_4 \mu_I \mu_4 (\beta_H L + d_H) - \mu_I (\beta_H L + d_H)[\mu_4 + (r_4 + \beta_4)L] - \kappa_I \rho r_4 \mu_4 V_i^* = 0.$$

We get the expression for $V_i^*$ in terms of the total viral load,

$$\begin{aligned} V_i^* = \frac{1}{\kappa_I \rho r_4 \mu_4}[&\beta_H \mu_I \mu_4 (r_4 + \beta_4)L - \beta_H \mu_I \mu_4 L - \mu_I (r_4 + \beta_4) d_H L - \beta_H \mu_I (r_4 + \beta_4) L^2 \\ &+ \mu_I \mu_4 d_H (\beta_4 - 1)]. \end{aligned} \tag{5.7}$$

Equation (5.7) shows that each viral strain $V_i^*$ has the same abundance at the endemic equilibrium, then the total viral load at equilibrium is

$$\begin{aligned} L &= \sum_{1}^{n} V_i^* = n V_i^* \\ &= \frac{n}{\kappa_I \rho r_4 \mu_4}[\beta_H \mu_I \mu_4 (r_4 + \beta_4)L - \beta_H \mu_I \mu_4 L - \mu_I (r_4 + \beta_4) d_H L - \beta_H \mu_I (r_4 + \beta_4) L^2 \\ &+ \mu_I \mu_4 d_H (\beta_4 - 1)]. \end{aligned} \tag{5.8}$$

Equation (5.8) is a quadratic equation,

$$f(L) = aL^2 + bL + c = 0, \tag{5.9}$$

where

$$a = \frac{\beta_H \mu_I (r_4 + \beta_4)}{\kappa_I \rho r_4 \mu_4}, \tag{5.10}$$

$$b = \frac{1}{\kappa_I \rho r_4 \mu_4}[\beta_H \mu_I \mu_4 (1 - r_4 - \beta_4) + \mu_I (r_4 + \beta_4) d_H] + 1/n, \tag{5.11}$$

$$c = \frac{\mu_I \mu_4 d_H (1 - \beta_4)}{\kappa_I \rho r_4 \mu_4}. \tag{5.12}$$

When $\mathcal{R}_0 = \beta_4 > 1$, because $a$ is positive and $c$ is negative, there exists a unique endemic equilibrium $L^*$.

We aim to analyze if the total viral load $L^*$ increases with an increasing number of viral strains. From the equation (5.9),

$$\frac{\partial f}{\partial L}\frac{\partial L}{\partial n} + \frac{\partial f}{\partial n} = 0, \tag{5.13}$$

and

$$\frac{\partial L}{\partial n} = -\frac{\partial f/\partial n}{\partial f/\partial L}. \tag{5.14}$$

At the unique endemic equilibrium $L^*$,

$$\frac{\partial f(L^*)}{\partial n} = -\frac{L^*}{n^2} < 0,$$

and

$$\frac{\partial f(L^*)}{\partial L} = 2aL^* + b > 0.$$

Thus,

$$\frac{\partial L^*}{\partial n} > 0. \tag{5.15}$$

The signs of $\partial T_4^*/\partial L$ and $\partial T_H^*/\partial L$ are used to show how CD4 T cells and total T helper cells are influenced by the total viral load, where

$$\frac{\partial T_4^*}{\partial L} = -\frac{\mu_4 (r_4 + \beta_4)}{[(r_4 + \beta_4)L + \mu_4]^2} < 0, \tag{5.16}$$

and

$$\frac{\partial T_H^*}{\partial L} = \frac{r_4\mu_4[\mu_4(\mu_H - p_H) - \beta_H(r_4+\beta_4)L^2]}{[(r_4+\beta_4)L+\mu_4]^2(\beta_H L + \mu_H - p_H)^2}. \tag{5.17}$$

Equations (5.15) and (5.16) illustrate that in the long asymptomatic stage, viral mutation might cause a high set-point viral load and a low CD4 T cell count. The rate of change of equilibrium T helper cells with respect to the total viral load ($\partial T_H^*/\partial L$) depends on the sign of

$$\mu_4(\mu_H - p_H) - \beta_H(r_4+\beta_4)L^2. \tag{5.18}$$

There exists a critical value $\hat{L}$ for the total viral load $L$, such that

$$\hat{L} = \sqrt{\frac{\mu_4(\mu_H - p_H)}{\beta_H(r_4+\beta_4)}}. \tag{5.19}$$

When the number of viral strains is large enough, i.e., $L^* > \hat{L}$, helper T cell load drops. If $L^* < \hat{L}$, the total helper T cells at equilibrium increases with an increasing number of viral strains because $\partial T_H^*/\partial L > 0$ and $\partial L^*/\partial n > 0$.

The HIV tests typically give the total CD4 T cell count, instead of differentiating $T_4$ and $T_H$. The total CD4 T cell count is given by

$$\frac{\partial T_4^*}{\partial L} + \frac{\partial T_H^*}{\partial L} = \frac{DL^{*2} + EL^* + F}{[(r_4+\beta_4)L^*+\mu_4]^2(\beta_H L^* + \mu_H - p_H)^2}, \tag{5.20}$$

where

$$D = -(r_4+1)\mu_4\beta_H(r_4+\beta_4), \tag{5.21}$$

$$E = -2\mu_4\beta_H(r_4+\beta_4)(\mu_H - p_H), \tag{5.22}$$

$$F = \mu_4(\mu_H - p_H)[r_4\mu_4 - (\mu_H - p_H)(r_4+\beta_4)]. \tag{5.23}$$

If $F < 0$, $\partial T_4^*/\partial L + \partial T_H^*/\partial L$ is always negative, which means that the total T cells is a negative function of the number of viral strains. When $F > 0$, there is a critical value $\tilde{L} = (-E - \sqrt{E^2 - 4DF})/2D$. If $L^* < \tilde{L}$, then $\partial T_4^*/\partial L + \partial T_H^*/\partial L > 0$, whereas if $L^* > \tilde{L}$, then $\partial T_4^*/\partial L + \partial T_H^*/\partial L < 0$. Because $\partial L^*/\partial n > 0$, if $L^* < \tilde{L}$, then the total CD4 T cell count increases with viral diversity, and if $L^* > \tilde{L}$, then the count decreases.

## 5.3 Simulations

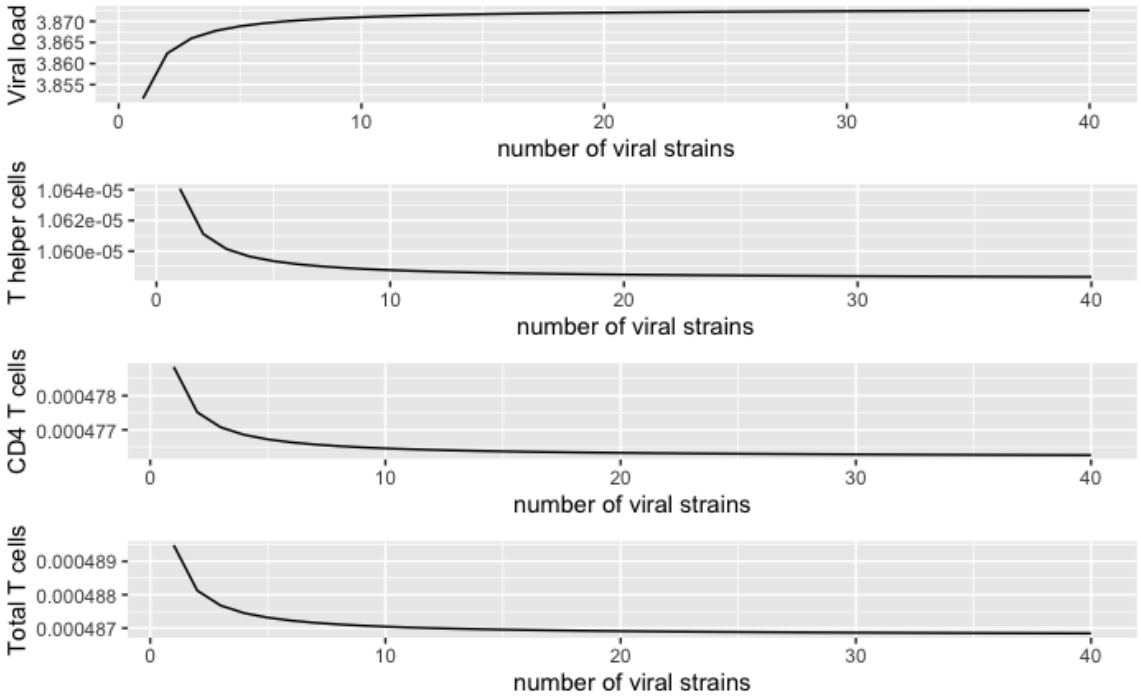


Figure 5.1: The total viral load, total helper T cells, naive CD4 T cells and total CD4 T cells versus number of virus strains for model (5.2), where $\mu_4 = 3.875$, $\beta_4 = 1575$, $\beta_H = 23625$, $r_4 = 525$, $\kappa_I\rho = 2025.625$, $\mu_I = 3.875$, $\mu_H = 3.875$, $p_H = 1.5$. Most parameter values from Hogue et al. [9] except $\kappa_I\rho$.

In the simulations, the values of parameters except $\kappa_I\rho$ used in Figure 5.1 are taken from the Hogue et al. model [9]. First of all, we compute the endemic equilibrium of the population size of virus by solving the quadratic equation (5.9). Then we obtain the endemic equilibrium of naive CD4 T cells and helper T cells from the equations (5.3a) and (5.3b). Figure 5.1 shows that the total viral load at equilibrium increases with increasing viral diversity, while total helper T cells and naive CD4 T cells decrease. In Figure 5.1, $\mathcal{R}_0 = \beta_4 = 1575$ and $\beta_H = 23625$. Parameter values used in Figure 5.1 give $\mu_4(\mu_H - p_H) - \beta_H(r_4 + \beta_4)L^{*2}$ always negative for positive $L^*$, and the coefficient $F$ in equation (5.23) is always negative when $n < 40$. Because $\mathcal{R}_0 = \beta_4 = 1575$ is large and unrealistic, we choose a smaller value of $\beta_4$ and $\beta_H$ to generate

Figure 5.2. When $\beta_4 = 1.575$ and $\beta_H = 23.625$, $\mu_4(\mu_H - p_H) - \beta_H(r_4 + \beta_4)L^{*2} > 0$ and $dT_4^*/dL + dT_H^*/dL > 0$ when $n \leq 22$. Figure 5.2 shows peaks in helper T cells and total T cells around $n = 22$. Viral load grows gradually when $n \leq 22$, then increases dramatically. Figure 5.3 is generated with $\mathcal{R}_0 = \beta_4 = 1.575$ and $\beta_H = 1.8375$. Figure 5.3 shows that when $\beta_4$ and $\beta_H$ are small enough, i.e.,

$$\mu_4(\mu_H - p_H) - \beta_H(r_4 + \beta_4)L^{*2} > 0,$$

then T helper cells increase with the number of viral strains.

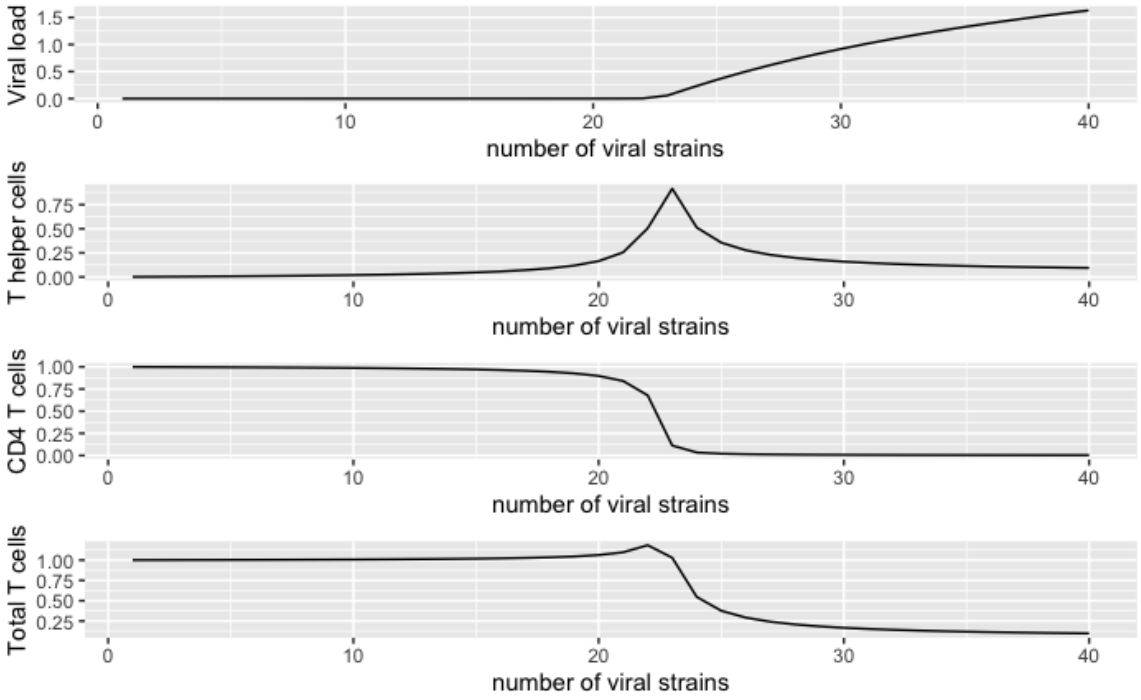


Figure 5.2: The total viral load, total helper T cells, naive CD4 T cells and total CD4 T cells versus number of virus strains for model (5.2), where $\mu_4 = 3.875$, $\beta_4 = 1.575$, $\beta_H = 23.625$, $r_4 = 525$, $\kappa_I\rho = 2025.625$, $\mu_I = 3.875$, $\mu_H = 3.875$, $p_H = 1.5$.

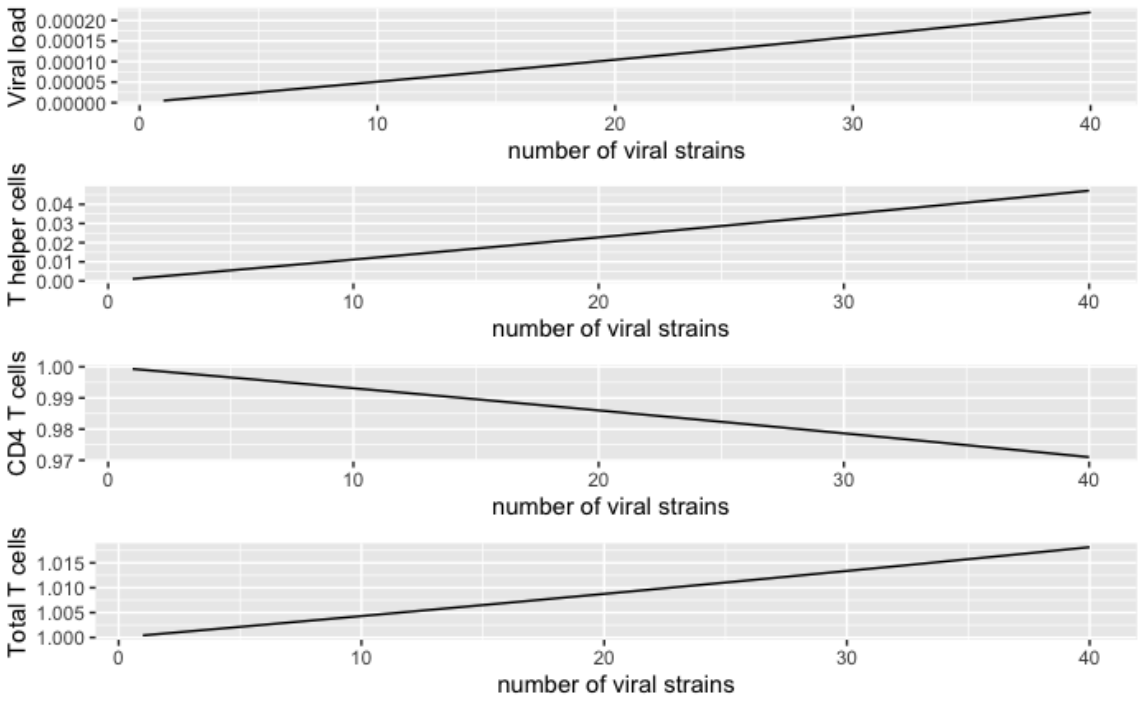


Figure 5.3: The total viral load, total helper T cells, naive CD4 T cells and total CD4 T cells versus number of virus strains for model (5.2), where $\mu_4 = 3.875$, $\beta_4 = 1.575$, $\beta_H = 1.8375$, $r_4 = 525$, $\kappa_I \rho = 2025.625$, $\mu_I = 3.875$, $\mu_H = 3.875$, $p_H = 1.5$.

## 5.4 Concluding Remarks

In this chapter, we considered the effect of viral diversity on the equilibrium viral load and CD4 T cell counts, using a more realistic HIV model from Chapter 2 than the ones in Chapter 4. We incorporated viral strains into the model (2.3). We demonstrated that increasing the population size of the virus resulting from viral diversity might cause CD4 T cells depletion. Moreover, the rate of change of helper T cells with respect to the viral load ($\partial T_H^*/\partial L$) at the steady state depends on the infection rate of CD4 T cells and helper T cells ($\beta_4$ and $\beta_H$), and the total viral load ($L^*$). When $\beta_4$ and $\beta_H$ are small enough, the total load of helper T cells initially increases with viral load. However, with an increasing number of viral strains and viral load, total helper T cells grow to a peak, and then decrease. The model (5.2) does not exhibit

a viral diversity threshold, the endemic equilibrium of the virus is always bounded. However, unlike model (4.9), this model does not always show that virus grows faster with viral diversity. Further investigation is needed to understand what modifications are needed for our model to agree with data.

# Chapter 6

# Conclusions

In this thesis, we generated a within-host HIV model to analyze the viral dynamics at the acute stage. The Hogue et al. model [9] illustrates the dual role of dendritic cells in the study of HIV, dendritic cells not only prime CTLs, but also activate CD4 T cells to become helper T cells. We simplified the Hogue et al. model [9] and only considered the dynamics of CD4 T cells, helper T cells, infected cells and viral load. Although helper T cells are the second susceptible class, they have no influence on the basic reproduction number $\mathcal{R}_0$. We found that a large infection rate of helper T cells or a large activation rate of CD4 T cells may cause backward bifurcation. On the other hand, a larger load of CTLs can prevent the existence of backward bifurcation. This model assumed that the CTL population is proportional to the viral load, and an extended model with CTL dynamics numerically shows that backward bifurcation may still occur.

Then we generated an extended model that contains a latently infected class. Because we focus on the viral dynamics at the acute stage, long-lived latency is not considered in our model. We study only the latent infection of naive CD4 T cells, rather than the resting CD4 T cells. The basic reproduction number $\mathcal{R}_0$ increases with the activation from latent infections by other pathogens ($\sigma$). The backward bifurcation condition for this model has a dependence similar to our 4-dimensional model on the load of CTLs, the infection rate of helper T cells and the activation rate

of CD4 T cells.

We analytically derived the backward bifurcation conditions, but the stability of endemic equilibria are only explored numerically. It would be an interesting future research project to analytically study the stability of the endemic equilibria. Our numerical analysis does not show Hopf bifurcation of an endemic equilibrium when $\mathcal{R}_0 > 1$. The model used by Pankavich et al. [16] exhibits Hopf bifurcation because their model uses a saturation activation term for CD4 T cells. With a bilinear activation term as in model (2.3), Hopf bifurcation cannot occur in their model.

In this thesis, we did not take drug therapy into consideration. However, our models suggest that decreasing the reproduction number below 1 by drug therapy may not control the spread of HIV within the host. If backward bifurcation occurs, it may be necessary to reduce the reproduction number below $\mathcal{R}_C$. Otherwise if $\mathcal{R}_C < \mathcal{R}_0 < 1$, a large initial viral load may still lead to the infection of HIV, whereas for a small initial viral load, HIV dies out.

The second purpose of this thesis is to investigate the progression to AIDS caused by viral diversity. A simple model generated by Wodarz and Nowak [27] is concerned with multiple viral strains, strain-specific immune responses against each viral strain and group-specific immune responses against all viral strains. Their model shows a threshold for viral diversity, the viral population is able to escape from the control of the immune responses if the number of viral strains exceeds this threshold. We found that the progression to AIDS may be caused by viral diversity with or without group-specific immune responses. By adding density dependence to the viral load, we showed that the threshold no longer exists, and the viral load increases with the number of viral strains.

The Wodarz and Nowak model [27] ignores important features, such as CD4 T cells and helper T cells. We added viral diversity in our 4-dimensional model (2.2) to illustrate the effect of viral diversity on CD4 T cells and helper T cells. Our model (5.2) suggests that the total viral load is bounded and is an increasing function of the number of viral strains, while CD4 T cells decrease with viral strains. However, this

model shows that helper T cells and total T cells (the sum of CD4 T cells and helper T cells) may increase or decrease with viral diversity depending on the parameter values. When the infection rate of CD4 T cells ($\beta_4$) or helper T cells ($\beta_H$) is small, helper T cells count is an increasing function of total viral load and viral diversity. On the other hand, empirical data show that the total CD4 T cell count always decreases as a patient progress to AIDS [15]. Thus our model demonstrates that viral diversity does not fully explain the progression to AIDS. A more sophisticated model may be needed to understand the progression to AIDS.

# Bibliography

[1] C. Castillo-Chavez and B. Song. Dynamical models of tuberculosis and their applications. *Mathematical Biosciences*, 1:361–404, 2004.

[2] L. Chavez, V. Calvanese, and E. Verdin. HIV latency is established directly and early in both resting and activated primary CD4 T cells. *PLoS Pathogens*, 11:e1004955, 2015.

[3] R. V. Culshaw, S. Ruan, and R. J. Spiteri. Optimal HIV treatment by maximising immune response. *Journal of Mathematical Biology*, 48(5):545–562, 2004.

[4] H. M. Doekes, C. Fraser, and K. A. Lythgoe. Effect of the latent reservoir on the evolution of HIV at the within- and between-host levels. *PLoS Computational Biology*, 13, 2017.

[5] M. M. Hadjiandreou, R. Conejeros, and V. S. Vassiliadis. Towards a long-term model construction for the dynamic simulation of HIV infection. *Mathematical Biosciences*, 4(3):489–504, 2007.

[6] M. M. Hadjiandreou, R. Conejeros, and D. I. Wilson. Long-term HIV dynamics subject to continuous therapy and structured treatment interruptions. *Chemical Engineering Science*, 64:1600–1617, 2009.

[7] E. A. Hernandez-Vargas and R. H. Middleton. Modeling the three stages in HIV infection. *Journal of Theoretical Biology*, 320:33–40, 2013.

[8] A. L. Hill. Mathematical models of HIV latency. *Curr Top Microbiol Immunol*, 417:131–156, 2019.

[9] I. B. Hogue, S. H. Bajaria, B. A. Fallert, S. Qin, T. A. Reinhart, and D. E. Kirschner. The dual role of dendritic cells in the immune response to HIV-1 infection. *The Journal of General Virology*, 89(Pt 9):2228, 2008.

[10] S. Iwami, S. Nakaoka, Y. Takeuchi, Y. Miura, and T. Miura. Immune impairment thresholds in HIV infection. *Immunology Letters*, 123(2):149–154, 2009.

[11] H. Y. Lee, D. J. Topham, S. Y. Park, J. Hollenbaugh, J. Treanor, T. R. Mosmann, X. Jin, B. M. Ward, H. Miao, and J. Holden-Wiltse. Simulation and prediction of the adaptive immune response to influenza A virus infection. *Journal of Virology*, 83(14):7151–7165, 2009.

[12] J. Luo, W. Wang, H. Chen, and R. Fu. Bifurcation of a mathematical model for HIV dynamics. *Journal of Mathematical Analysis and Applications*, 434:837–857, 2016.

[13] K. A. Lythgoe, L. Pellis, and C. Fraser. Is HIV short-sighted? Insights from a multistrain nested model. *Evolution*, 67(10):2769–2782, 2013.

[14] M. A. Nowak and R. M. May. Virus dynamics. mathematical principles of immunology and virology. *Oxford:Oxford University Press*, 2000.

[15] A. A. Okoye and L. J. Picker. CD4 T cell depletion in HIV infection: mechanisms of immunological failure. *Immunological reviews*, 254:54–64, 2013.

[16] S. Pankavich, N. Neri, and D. Shutt. Bistable dynamics and Hopf bifurcation in a refined model of early stage HIV infection. *Discrete and Continuous Dynamical Systems Series B*, 25:2867–2893, 2020.

[17] A. S. Perelson and R. M. Ribeiro. Modeling the within-host dynamics of HIV infection. *BMC Biology*, 11(1):96, 2013.

[18] C. Qin, X. Wang, and L. Rong. An age-structured model of HIV latent infection with two transmission routes: analysis and optimal control. *Complexity*, 2020.

[19] A. Rambaut, D. Posada, K. A. Crandall, and E. C.Holmes. The causes and consequences of HIV evolution. *Nature Reviews*, 5:52–61, 2004.

[20] L. Rong and A. S. Perelson. Modeling HIV persistence, the latent reservoir, and viral blips. *Journal of Theoretical Biology*, 260:308–331, 2009.

[21] L. Rong and A. S. Perelson. Modeling latently infected cell activation: viral and latent reservoir persistence, and viral blips in HIV-infected patients on potent therapy. *PLoS Computation Biology*, 5, 2009.

[22] R. F. Siliciano and W. C. Greene. HIV latency. *Cold Spring Harbor perspectives in medicine*, 1(1):a007096, 2011.

[23] M. Stevenson, T. L. Stanwick, M. P. Dempsey, and C. A. Lamonica. HIV-1 replication is controlled at the level of T cell activation and proviral integration. *The EMBO Journal*, 9:1551–1560, 1990.

[24] P. van den Driessche and J. Watmough. Reproduction numbers and sub-threshold endemic equilibria for compartmental models of disease transmission. *Mathematical Biosciences*, 28(48):29–48, 2002.

[25] Y. Wang, Y. Zhou, F. Brauer, and J. M. Heffernan. Viral dynamics model with CTL immune response incorporating antiretroviral therapy. *Journal of Mathematical Biology*, 67(4):901–934, 2013.

[26] D. Wodarz, A. L. Lloyd, V. A. Jansen, and M. A. Nowak. Dynamics of macrophage and T cell infection by HIV. *Journal of Theoretical Biology*, 196:101–113, 1999.

[27] D. Wodarz and M. A. Nowak. Mathematical models of HIV pathogenesis and treatment. *BioEssays*, 24(12):1178–1187, 2002.

[28] X. Xie, J. Ma, and P. van den Driessche. Backward bifurcation in within-host HIV models. *Mathematical Biosciences*, 335:108569, 2021.